CORA Cork Open Research Archive
Cartlann Taighde Oscailte Chorcaí

Title	Paths from stationary to chaos in passively mode-locked fiber lasers: research progress of soliton pulsations and soliton explosions
Authors	Han, Ying;Gao, Bo;Hao, Yabin;Ponraj, Joice Sophia;Ma, Chunyang;Huo, Jiayu;Wu, Ge;Li, Yingying;Al-Amoudi, Bashaer Omar;Wageh, S.;Al-Ghamdi, Ahmed A.;Liu, Lie;Zhang, Han
Publication date	2022-09-14
Original Citation	Han, Y., Gao, B., Hao, Y., Ponraj, J. S., Ma, C., Huo, J., Wu, G., Li, Y., Al-Amoudi, B. O., Wageh, S., Al-Ghamdi, A. A., Liu, L. and Zhang, H. (2022) 'Paths from stationary to chaos in passively mode-locked fiber lasers: research progress of soliton pulsations and soliton explosions', Journal of Physics B: Atomic, Molecular and Optical Physics, 55(22), 222001 (25pp). https://doi.org/10.1088/1361-6455/ac9204
Type of publication	Article (peer-reviewed)
Link to publisher's version	10.1088/1361-6455/ac9204
Rights	© 2022, IOP Publishing Ltd. This is an author-created, un-copyedited version of an article accepted for publication in Journal of Physics B: Atomic, Molecular and Optical Physics. The publisher is not responsible for any errors or omissions in this version of the manuscript or any version derived from it. The Version of Record is available online at: https://iopscience.iop.org/article/10.1088/1361-6455/ac9204 - https://creativecommons.org/licences/by-nc-nd/3.0
Download date	2026-11-15 11:26:11
Item downloaded from	https://hdl.handle.net/10468/13624



University College Cork, Ireland
Coláiste na hOllscoile Corcaigh

Journal of Physics B: Atomic, Molecular and Optical Physics

ACCEPTED MANUSCRIPT

Paths from stationary to chaos in passively mode-locked fiber lasers: research progress of soliton pulsations and soliton explosions

To cite this article before publication: Ying Han *et al* 2022 *J. Phys. B: At. Mol. Opt. Phys.* in press https://doi.org/10.1088/1361-6455/ac9204

Manuscript version: Accepted Manuscript

Accepted Manuscript is "the version of the article accepted for publication including all changes made as a result of the peer review process, and which may also include the addition to the article by IOP Publishing of a header, an article ID, a cover sheet and/or an 'Accepted Manuscript' watermark, but excluding any other editing, typesetting or other changes made by IOP Publishing and/or its licensors"

This Accepted Manuscript is **© 2022 IOP Publishing Ltd**.

During the embargo period (the 12 month period from the publication of the Version of Record of this article), the Accepted Manuscript is fully protected by copyright and cannot be reused or reposted elsewhere.
As the Version of Record of this article is going to be / has been published on a subscription basis, this Accepted Manuscript is available for reuse under a CC BY-NC-ND 3.0 licence after the 12 month embargo period.

After the embargo period, everyone is permitted to use copy and redistribute this article for non-commercial purposes only, provided that they adhere to all the terms of the licence https://creativecommons.org/licences/by-nc-nd/3.0

Although reasonable endeavours have been taken to obtain all necessary permissions from third parties to include their copyrighted content within this article, their full citation and copyright line may not be present in this Accepted Manuscript version. Before using any content from this article, please refer to the Version of Record on IOPscience once published for full citation and copyright details, as permissions will likely be required. All third party content is fully copyright protected, unless specifically stated otherwise in the figure caption in the Version of Record.

View the article online for updates and enhancements.

This content was downloaded from IP address 86.44.130.187 on 21/09/2022 at 09:50

IOP Publishing Journal of Physics B: Atomic, Molecular and Optical Physics
Journal **XX** (XXXX) XXXXXX https://doi.org/XXXX/XXXX

Paths from stationary to chaos in passively mode-locked fiber lasers: research progress of soliton pulsations and soliton explosions

Ying Han,[1&] Bo Gao,[1a] Yabin Hao,[2&] Joice Sophia Ponraj,[3,4&] Chunyang Ma,[2,5] Jiayu Huo,[1] Ge Wu,[6] Yingying Li,[1] Bashaer Omar Al-Amoudi,[7] S. Wageh,[7] Ahmed A. Al-Ghamdi,[7] Lie Liu,[1] and Han Zhang[2a]

[1]College of Communication Engineering, Jilin University, Changchun 130012, PR China
[2]International Collaborative Laboratory of 2D Materials for Optoelectronics Science and Technology of Ministry of Education, College of Physics and Optoelectronic Engineering, Shenzhen University, Shenzhen 518060, PR China
[3]Physics Department, University College Cork, T12 XF62 Cork, Ireland
[4]Integrated Photonics Group, Tyndall National Institute, Lee Maltings, T12 R5CP Cork, Ireland
[5]Research Center of Circuits and Systems, Peng Cheng Laboratory, Shenzhen 518055, Guangdong, PR China
[6]College of Electronic Science and Engineering, Jilin University, Changchun 130012, PR China
[7]Department of Physics, Faculty of Science, King Abdulaziz University, Jeddah 21589, Saudi Arabia
[&]These authors contributed equally to this work and should be considered co-first authors.

E-mail: [1a)]Bo Gao: gaobo0312@jlu.edu.cn
[2a)]Han Zhang: hzhang@szu.edu.cn

Received xxxxxx
Accepted for publication xxxxxx
Published xxxxxx

Abstract

Research has shown that passively mode-locked fiber lasers produce chaotic output, which has caught the attention of physicists, chemists, and bio-scientists owing to their wide bandwidth, good random characteristics, and strong anti-interference. In passively mode-locked fiber lasers, soliton pulsations and soliton explosions with period bifurcation characteristics have been demonstrated to be effective paths to chaos as far as 20 years ago. However, due to the lack of real-time spectrum measurement techniques, the earlier research investigated their theoretical aspect. In recent years, the rise of the dispersive Fourier transform technique has activated an upsurge of experimental research. The present work first discussed the theoretical model of passively mode-locked fiber lasers, the computational analysis method of soliton dynamics, and the related theory of the dispersive Fourier transform technique. In addition, we presented and evaluated the progress of the theoretical and experimental research on soliton pulsations as well as on soliton explosions in passively mode-locked fiber lasers. Finally, we proposed the future research directions of the soliton pulsations and soliton explosions that offer great promise for scientific discoveries.

Keywords: soliton explosions, soliton pulsations, passively mode-locked fiber lasers, dispersive Fourier transform (DFT) technique

Accepted Manuscript

 © xxxx IOP Publishing Ltd

1. Introduction

In the early 1960s, Lorenz studied the atmospheric convection model, simplified the parameters, and established differential equations to simulate meteorological changes on the computer. He discovered that there is a nonlinear connection between the three time-varying parameters [1], and thus discovered the phenomenon of chaos in nature, Lorenz is praised as "the father of chaos". In aftermath of the first laser, researchers found the laser peak effect and the jump mode in some experiments, the earliest discovery of optical chaos. However, due to the limited understanding of optical chaos at that time, they based their explanation upon the theory of relaxation oscillation. In 1980, T. Yamada et al. proposed that increasing the degree of freedom in the laser can realize chaotic output [2]. As an example, semiconductor lasers can realize chaotic output through the method of external optical feedback [3-6]. In addition, the nonlinear Kerr effect contributes to the chaotic output of fiber lasers [7]. With the development of modern science and technology, chaos has gradually developed into a research hotspot and an important branch of nonlinear dynamics that is widely used in all walks of life. Contributed to its wide bandwidth, good random characteristics, and strong anti-interference characteristics [8], chaotic lasers are extensively employed in the field of chaotic radar ranging [9], chaotic secure communication [10], and fast physical random number generator [11].

Optical solitons refer to the wave whose shape, amplitude, and velocity remain unchanged during propagation. Optical solitons exist in many systems, such as Bose-Einstein condensates [12], coherent atomic media [13, 14, 15], solid lasers [16], and fiber lasers [17], which illustrates the universality of optical solitons. Fiber lasers gained attention and developed rapidly after they were realized because of their superiority such as simple structure, easy collimation, and flexible design [18]. Among them, passively mode-locked fiber lasers have three preponderances [19, 20]. (1) It can generate the fs-level ultrashort soliton pulses originating from the balance between the group velocity dispersion effect and the self-phase modulation effect in fiber lasers. fs-level ultrashort soliton pulses are rarely achieved by other lasers [21, 22]. (2) In contrast to actively mode-locked fiber lasers, passively mode-locked fiber lasers require no regulators or external equipment in the cavity [23]. (3) Self-starting can be realized under appropriate parameters [24]. The application of ultrafast passively mode-locked fiber lasers involves laser precision processing, laser marking, selective cutting, welding, medical treatment, and bioengineering [25-28]. In national defense and military, it can be applied to positioning, ranging, tracking, guidance, laser nuclear fusion, deep space laser communication, and simulated shooting [29-31]. It forms the essential tool in nonlinear optics, biochemistry, and material physics, among others [32]. The development of ultrafast passively mode-locked fiber lasers has become a hot topic around the world due to their scientific importance and broad application. As a result, the study of the chaotic output of passively mode-locked fiber lasers is of utmost importance.

Several mature and effective criteria have been developed over decades of exploration by scholars to determine whether a system exhibits chaotic motion, which is an important foundation of chaos research [33]. A chaotic system can, for example, be assessed by analyzing the bifurcation diagram, the strange attractor, the Lyapunov exponent, the power spectrum, and Komogorov entropy. Studies have focused a great deal of attention on soliton pulsations and soliton explosions as soliton solutions of the cubic-quintic Ginzberg-landau equation, which are closely related to period bifurcations and are effective paths to chaos for passively mode-locked fiber lasers [34-38]. Since conventional instruments have measurement bandwidths and response speeds, the experimental analysis of soliton dynamics often involves non-real-time multi-averaging measurements. The experimental analysis of soliton pulsations and soliton explosions is a great challenge, which is why early research focused mostly on theoretical analysis. Since the advent of the dispersive Fourier transform (DFT) technique for spectrum measurement in recent years, the bottleneck in the research on real-time spectrum characteristics has been broken, and great progress has been made in the experimental study of soliton pulsations and soliton explosions [39]. Research of this kind provides a means for people to study the chaotic output of passively mode-locked fiber lasers, deepens their understanding of the soliton dynamic characteristics, and provides a reference for the construction of the required stationary and chaotic laser output.

The in-depth analysis of the theoretical and experimental research progress of soliton pulsations and soliton explosions in passively mode-locked fiber lasers has been presented in this review. We briefly discussed the theoretical underpinnings of passively mode-locked fiber lasers in section 2, which include the nonlinear Schrödinger equation as well as its extended form, the cubic-quintic Ginzberg-landau equation, and their computational analysis methods (moment method, variational method, split-step Fourier method, and fourth-order Runge-Kutta method). Next, we demonstrated the principle, data collection, and data processing of the DFT technique. In section 3 and section 4, we presented advances in the study of soliton pulsations and soliton explosions in passively mode-locked fiber lasers, respectively. Each section is addressed separately into theoretical research and experimental research. Theoretical research can be summarized as soliton pulsations and soliton explosions in a continuous model based on the cubic-quintic Ginzberg-landau equation, and in a lumped model based on the nonlinear Schrödinger equation. In the experimental research aspects,

Accepted Manuscript

section 3 analyzed the research progress of single soliton pulsations and their self-organization (multi-soliton pulsations), and section 4 presented the research progress of typical soliton explosions and periodic soliton explosions in passively mode-locked fiber lasers. And the present work concluded with the prospects and future research directions in section 5.

2. Introduction of theoretical model and the DFT technique

2.1 Theoretical analysis method of passively mode-locked fiber lasers

2.1.1 Transmission equations

(1) Complex cubic-quintic Ginzberg-landau equation

A continuous model based on the cubic-quintic Ginzberg-landau equation (CQGLE) can be used to model the passively mode-locked fiber lasers to analyze soliton dynamics [40]. Nevertheless, there are a few difficulties in the application of rich types of soliton solutions in CQGLE, to be specific, certain soliton solutions only exist when there is a specific algebraic correlation between the parameters in equations, and other solutions can only be found using numerical methods. Due to the rich branch structure of solutions, it is very difficult to find accurate analytical solutions, but the approximate approach is still advisable. The complex CQGLE not only includes the effect of dispersion and dissipation but also considers the exchange of energy and the influence of high-order nonlinear effects. Specifically, it includes the cubic nonlinear term and quintic nonlinear term, the effects of self-steepness (SS), self-frequency shift, and third-order dispersion (TOD). Its one-dimensional master equation can be expressed as follows:

$$\frac{\partial U}{\partial Z} = \sum_{m\geq 2} \frac{i^{m+1}}{m!} \frac{\beta_m \partial^m U}{\partial T^m} + i\gamma |U|^2 U + (i\mu + \nu)|U|^4 U + \varepsilon |U|^2 U + gU + \beta \frac{\partial^2 U}{\partial T^2} \quad (1)$$

Table 1 lists the parameters and their abbreviation used in the equations of section 2.1.1. There are six system parameters in equation (1) where all units are normalized and dimensionless and it takes a considerable amount of calculation to find out the soliton solutions. Researchers have not fully grasped the region of soliton solutions until now. The initial approach is to find the parameter region with physical significance where the soliton solutions exist. After a stable local solution is found for the given parameters of the equation, it can be used as an initial condition to find the solutions for neighboring parameter values. By moving slowly through the parameter space, the region where soliton solutions exist can be found in a relatively simpler way.

Table 1. Parameters and their abbreviation in equations of section 2.1.1.

Parameters	Abbreviation
U	Slowly varying envelope of pulses
Z	Transmission length (proportional to the number of roundtrips)
ν	Fifth-order Kerr effect corresponds to the saturation of linear power as it is taken as the negative value
g	Gain of the doped-fiber
ε	The nonlinear gain caused by the saturated absorption effect
β	The spectral filter term
μ	The quintic nonlinear gain
α	Loss
$\beta_m = \frac{d^m \beta}{d\omega^m}\|_{\omega=\omega_0}$	m-order dispersion coefficient, ω and ω_0 are the frequency and center frequency of pulses, respectively
$T = t - z / v_g - \beta_1 z$	The time coordinate in the reference frame moves with the pulse at the group velocity v_g
$\|U\|^2$	Optical intensity
γ	Fiber nonlinear coefficient
T_R	Raman coefficient
g_0	Small signal gain
ω	Frequency of the incident pulse
Ω_g	Gain bandwidth of the doped fiber
E_{pulse}	Pulse energy
E_{sat}	Gain saturation energy

(2) Nonlinear Schrödinger equation and its extended form

The generalized nonlinear Schrödinger equation (GNLSE) can be derived directly from Maxwell's equations

Accepted Manuscript

under the assumption that the transient nonlinear polarization and the slowly varying envelope of pulses. GNLSE can be used to describe the soliton evolution in the un-doped fiber, such as the single-mode fiber (SMF) or the dispersion compensation fiber (DCF):

$$\frac{\partial U}{\partial Z} = -\frac{\alpha}{2}U + \sum_{m\geq 2}\frac{i^{m+1}}{m!}\frac{\beta_m \partial^m U}{\partial T^m} + i\gamma\{|U|^2 U + \frac{i}{\omega_0}\frac{\partial}{\partial T}(|U|^2 U) - T_R U\frac{\partial |U|^2}{\partial T}\} \quad (2)$$

The last three terms on the right side of equation (2) represent the effects of self-phase modulation (SPM), SS, and intra-cavity Raman scattering (IRS) in the fiber. By ignoring α, SS, and IRS in equation (2), it can be simplified to only include the dispersion effect and the SPM effect to describe the soliton evolution in the un-doped fiber, namely the nonlinear Schrödinger equation (NLSE) [41, 42]:

$$\frac{\partial U}{\partial Z} = \sum_{m\geq 2}\frac{i^{m+1}}{m!}\frac{\beta_m \partial^m U}{\partial T^m} + i\gamma |U|^2 U \quad (3)$$

Fiber lasers normally use rare-earth metal ion-doped fiber as the gain medium to provide the required gain for lasers, wherein the gain coefficient can be expressed as:

$$g(\omega) = \frac{g_0}{1 + (\omega / \Omega_g) + (E_{pulse} / E_{sat})} \quad (4)$$

The parameters and their abbreviation of equation (4) are listed in Table 1. The soliton evolution in doped-fiber (gain fiber) is analyzed by the Ginzberg-landau equation (GLE), which takes into account the effects of gain and gain dispersion:

$$\frac{\partial U}{\partial Z} = -\frac{\alpha}{2}U + \sum_{m\geq 2}\frac{i^{m+1}}{m!}\frac{\beta_m \partial^m U}{\partial T^m} + i\gamma |U|^2 U + \frac{g}{2}U + \frac{g}{2\Omega_g^2}\frac{\partial^2 U}{\partial T^2} \quad (5)$$

It can be seen that if α and g in equation (5) are considered as zero, the GLE becomes NLSE.

The above-mentioned NLSEs and GLEs only include the pulse evolution with one polarization direction in the fiber. Considering the birefringence effect and cross-phase modulation (XPM) effect of the fiber that exists in practical applications, two orthogonal polarization directions must be simultaneously included. In this case, GLEs need to be expanded into coupled GLEs:

$$\frac{\partial u}{\partial Z} = -\frac{\alpha}{2}u + i\beta u - \delta\frac{\partial u}{\partial T} + \sum_{m\geq 2}\frac{i^{m+1}}{m!}\frac{\beta_m \partial^m u}{\partial T^m} + i\gamma(|u|^2 + \frac{2}{3}|v|^2)u + \frac{i\gamma}{3}v^2 u^* + \frac{g}{2}u + \frac{g}{2\Omega_g^2}\frac{\partial^2 u}{\partial T^2}) \quad (6)$$

$$\frac{\partial v}{\partial Z} = -\frac{\alpha}{2}v + i\beta v - \delta\frac{\partial v}{\partial T} + \sum_{m\geq 2}\frac{i^{m+1}}{m!}\frac{\beta_m \partial^m v}{\partial T^m} + i\gamma(|v|^2 + \frac{2}{3}|u|^2)v + \frac{i\gamma}{3}u^2 v^* + \frac{g}{2}v + \frac{g}{2\Omega_g^2}\frac{\partial^2 v}{\partial T^2}) \quad (7)$$

u and v represent the amplitude of the two orthogonal polarization components, $2\beta = 2\pi\Delta n / \lambda$ is the wavenumber difference between them; $2\delta = 2\beta\lambda / 2\pi c$ represents the reciprocal of the v_g difference.

2.1.2 Calculation methods

Nonlinear differential equations are the mathematical basis of soliton theory, by which one can get soliton solutions of equations through analytical methods or numerical methods. The common analytical methods include the inverse scattering method [43, 44], the Hirota bilinear method [45, 46], the Bäcklund transform [47], and other perturbation methods [48, 49]. However, due to its limitations, it is exceptionally uncommon to obtain soliton solutions by analytical methods. The Fourier transform method, Runge-Kutta method, pseudospectral method, and other numerical methods have become very essential and widespread methods for obtaining soliton solutions. The Fourier transform method with the advantages of simple principle, high efficiency, and ease of programming, which transforms a signal from the time domain to the frequency domain, has a wide range of applications in acoustics, telecommunications, and signal processing. In practical applications, the fast Fourier transform algorithm, which may reduce the quantity of calculation and increase the speed of calculation, has been widely promoted. The analytical methods and numerical methods will be briefly discussed in the following part.

(1) Analytical methods: moment method and variational method

The complex CQGLE is different from the integrable NLSE as well as its extended form. Its accurate soliton solutions cannot be obtained by the inverse scattering method. With the use of analytical methods such as the moment method or variational method, it is often necessary to introduce ansatz solitons or additional approximate conditions to deal with CQGLE, and the core idea is to transform the problem of infinite dimensions into finite dimensions. Equation (1) is rewritten into equation (8) for the convenience of explanation:

$$i\frac{\partial U}{\partial Z} - \beta\frac{\partial^2 U}{\partial T^2} + \gamma |U|^2 U + \sum_{m\geq 2}\frac{i^{m+1}}{m!}\frac{\beta_m \partial^m U}{\partial T^m} = i[\alpha\frac{\partial |U|^2}{\partial T} + \varepsilon |U|^2 U - (i\mu + \nu)|U|^4 U] \quad (8)$$

For the convenience of the following description, the terms on the right side of equation (8) are set as $R[u]$, that is

$$R[U] = i[\alpha\frac{\partial |U|^2}{\partial T} + \varepsilon |U|^2 U - (i\mu + \nu)|U|^4 U] .$$

The moment method needs to introduce five moments [50]:

$$\begin{cases} Q = \int_{-\infty}^{+\infty} |U|^2 dT \\ P = 0.5\int_{-\infty}^{+\infty} (UU_T^* - U^* U_T) dT \\ I_1 = \int_{-\infty}^{+\infty} T|U|^2 dT \\ I_2 = \int_{-\infty}^{+\infty} (T - t_0)^2 |U|^2 dT \\ I_3 = \int_{-\infty}^{+\infty} (T - t_0)(UU_T^* - U^* U_T) dT \end{cases} \quad (9)$$

Accepted Manuscript

t_0 is the centroid position of the ansatz solutions. In a non-conservative system, these moments satisfy the following differential equations:

$$\begin{cases} \frac{dQ}{dZ} = i\int_{-\infty}^{+\infty}(UR^* - U^*R)dT \\ \frac{dP}{dZ} = -i\int_{-\infty}^{+\infty}(U_T R^* + U_T^* R)dT \\ \frac{dI_1}{dZ} = -2i\beta P + i\int_{-\infty}^{+\infty} T(UR^* - U^*R)dT \\ \frac{dI_2}{dZ} = 2i\beta I_3 + \int_{-\infty}^{+\infty}(T - t_0)^2(UR^* - U^*R)dT \\ \frac{dI_3}{dZ} = 2P\frac{dt_0}{dZ} + i\int_{-\infty}^{+\infty}(4\beta|U_T|^2 + \gamma|U|^4)dT \\ +2i\int_{-\infty}^{+\infty}(T - t_0)^2(U_T R^* - U_T^* R)dT + i\int_{-\infty}^{+\infty}(UR^* + U^*R)dT \end{cases} \quad (10)$$

If combined with the ansatz solution of U, the infinite-dimensional differential equation (10) can be reduced to the finite-dimensional problem of each parameter in the ansatz solution, and each stable fixed point corresponds to a specific soliton solution.

The variational method needs researchers to construct the functional J, and treat the CQGLE as the Lagrangian equation under extreme conditions [51-53]:

$$J = \iint LdTdZ \rightarrow f_{CQGLE} = \frac{\delta L}{\delta U} \quad (11)$$

where $f_{CQGLE} = i\frac{\partial U}{\partial Z} - \beta\frac{\partial^2 U}{\partial T^2} + \gamma|U|^2 U - R[U]$.

For $\delta J = \iint \frac{\delta L}{\delta U}\delta U dTdZ = \iint(\frac{\delta L_{Ham}}{\delta y} - R[U])\delta U dTdZ$,

through the Ritz method, it can be further written as:

$$\begin{aligned} &\iint(\frac{\delta L_{Ham}}{\delta U} - R[U])\frac{\partial U}{\partial p}\delta p dTdZ = \\ &\iint(\frac{\delta L_{Ham}}{\delta U} - R[U]\frac{\partial U}{\partial p})\delta p dTdZ = \\ &\int(\int\frac{\delta L_{Ham}}{\delta U} - R[U]\frac{\partial U}{\partial p})dTdZ = 0 \end{aligned} \quad (12)$$

where $L_{Ham} = \frac{i}{2}(UU_Z^* - U^*U_Z) + \beta|U_T|^2 + \frac{\gamma}{2}|U|^4$ and p corresponds to each parameter in the ansatz solution. Note that (U,U^*), the last term of the equation (12) should be written as:

$$\int(\int\frac{\delta L_{Ham}}{\delta y} - R[U]\frac{\partial U}{\partial p}dT)\delta p dZ = \int(\int(\frac{\delta L_{Ham}}{\delta y} - R[U]\frac{\partial U^*}{\partial p} - R^*\frac{\partial U}{\partial p}))dT\delta p dZ \quad (13)$$

In other words, equation (12) results in a series of differential equations about the parameters in the ansatz solution. The next step is to analyze the stability of a dynamic system similar to the moment method.

These two types of analytical methods can be used in a wide range of situations and do not have stringent criteria for the master equation's form. The precision of the produced results, on the other hand, is dependent on the form of the ansatz solutions. That is, different ansatz solutions will present different calculation challenges, for example, hyperbolic secant and super-Gaussian functions are simple to integrate. Other complicated ansatz solutions make the whole computational process incredibly difficult.

(2) Numerical methods: split-step Fourier method and fourth-order Runge-Kutta algorithm

Numerical methods do not have too many requirements for the form of the master equation, which makes them very useful for analyzing the nonlinear dynamics in the fiber. Currently, the split-step Fourier method is the most often used approach to deal with the problem of pulse evolution in nonlinear dispersive media as it is reasonably fast compared to other algorithms. With the use of the split-step Fourier method, the equation (5) is usually rewritten as follows:

$$\frac{\partial U}{\partial Z} = (\hat{D} + \hat{N})U \quad (14)$$

$\hat{D}$ represents the linear operator of dispersion and loss of the nonlinear medium, and $\hat{N}$ is the nonlinear operator that determines the nonlinear effect. $\hat{D}$ and $\hat{N}$ are represented by equation (15) and equation (16), respectively:

$$\hat{D} = \sum_{m\geq 2}\frac{i^{m+1}}{m!}\frac{\beta_m\partial^m}{\partial T^m} - \frac{\alpha}{2} \quad (15)$$

$$\hat{N} = i\gamma[|U|^2 U + \frac{i}{\omega_0}\frac{\partial}{\partial T}(|U|^2 U - T_R U\frac{\partial|U|^2}{\partial T})] \quad (16)$$

When a pulse propagates through the fiber, the dispersion effect and nonlinear effects occur concurrently. It can be hypothesized that these two effects can independently alter the pulse evolution while passing a sufficiently tiny distance h, and thus achieve virtually accurate results, using the split-step Fourier method. In other words, introduce the pulse evolution from Z to $Z+h$ in two steps, the first step is to set $\hat{D} = 0$ to let the nonlinear work alone; the second step is to set $\hat{N} = 0$ where only dispersion exists, which can be expressed by the equation (17):

$$U(Z + h,T) \approx exp(h\hat{D})exp(h\hat{N})U(Z,T) \quad (17)$$

As required, the index part $exp(h\hat{D})$ is computed in the Fourier domain:

$$exp(h\hat{D})B(Z,T) \approx F_T^{-1}exp[(h\hat{D}(i\omega))]U(Z,T)F_T B(Z,T) \quad (18)$$

F_T and F_T^{-1} represent the Fourier transform and the inverse Fourier transform. Split-step Fourier method is relatively simple, however, to guarantee accuracy during the calculation

Accepted Manuscript

process, the value of *Z* and *T* must be appropriately selected. Choosing the best parameters is a complex matter. Generally speaking, as long as it is used carefully, the split-step Fourier method can be a very useful mathematical tool.

The fourth-order Runge-Kutta (RK4IP) method is a high-precision single-step algorithm widely used in engineering that can be used to solve differential equations. If regarded NLSE as $U_Z=f(Z, U)$, researchers could employ the RK4IP method to solve the initial value problem of NLSE with the initial condition of $U(0, T)$. The derivation part on the right side of the NLSE can be solved by the following high-order difference equation:

$$\frac{\partial^2 U(Z,T_i)}{\partial T^2} = \frac{-U(Z,T_{i+2}) + 16U(Z,T_{i+1}) - 30U(Z,T_i) + 16U(Z,T_{i-1}) - U(Z,T_{i-2})}{12\Delta^2} \quad (19)$$

T_i represents the discretization of the optical field $U(Z,T)$ in the time domain and Δ is the time domain sampling interval. The partial differential equations can be solved in two steps. For each point in the time window, solve the equation (19) and then apply the Runge-Kutta method to solve partial equations $\frac{\partial U(Z,T_i)}{\partial Z} = f(U(Z,T_i), A(0,t_i))$, which have the initial value problem.

The RK4IP method offers good accuracy and strong numerical stability, but its implementation principles and programming are complicated. The well-known first-order Euler equation can be written as:

$$\begin{cases} U_{n+1} = U_n + hK \\ K_1 = f(Z_n, U_n) \end{cases} \quad (20)$$

$U_n = U(Z_n, T)$ is the discretization of the optical field along the length of the fiber, h is the length of the sampling interval, and $f(Z_n, U_n)$ represents the right part of the NLSE. If the average value of the approximate slope K_1 at the point Zn and the approximate slope K_2 at the next point Z_{n+1} is used as the approximate average slope K_*, then we can obtain the improved Euler equation with second-order accuracy:

$$\begin{cases} U_{n+1} = U_n + h(K_1 + 2K_2) \\ K_1 = f(Z_n, U_n) \\ K_2 = f(Z_n + h, A_n + hK_1) \end{cases} \quad (21)$$

By analogy, if the slope values K_1, K_2...Km at multiple points are estimated multiple times in the interval of $[Z_n, Z_{n+1}]$, and these slope values are weighted and averaged, researchers could estimate the approximate value of K_*. Subsequently, a higher-order equation with higher accuracy is derived. By excluding the rigorous mathematical derivation, the well-known RK4IP equations can be given as:

$$\begin{cases} U_{n+1} = U_n + h(K_1 + 2K_2 + 2K_3 + K_4)/6 \\ K_1 = f(Z_n, U_n) \\ K_2 = f(Z_n + h/2, A_n + hK_1/2) \\ K_3 = f(Z_n + h/2, A_n + hK_2/2) \\ K_4 = f(Z_n + h/2, A_n + hK_3) \end{cases} \quad (22)$$

The output form of the optical field $U_n = (Z_n, T)$ transmitted through any length $Z=Zn$ can be obtained numerically by employing the above equations.

If the optical field and nonlinear are strong, the pulse envelope changes rapidly in the propagation direction, so it is necessary to shorten the step length *h* to improve the calculation accuracy. When compared to the split-step Fourier method, it is more obvious and simple to program using equations (20) and (22) directly if the derivation procedure of the Runge-Kutta equation is ignored. It is also convenient to use symmetric or periodic borders for the temporal window's boundary criteria. However, RK4IP has a flaw in that its operating speed is slower than the split-step Fourier method.

2.2 Real-time spectrum measurement technique: dispersive Fourier transform

To study the physical mechanism of the soliton pulsations and soliton explosions in the passively mode-locked fiber lasers, it is necessary to directly record the transient evolution of soliton pulses. Therefore, the testing techniques must meet three criteria. Testing methods should have sufficiently high enough time or spectral resolution and should be real-time to constantly record the dissipative structure. Furthermore, the time window of testing methods should be long enough, so it can record hundreds to thousands of pulse evolution roundtrips (RTs) at once. The scanning speed of traditional measuring instruments like autocorrelators and spectrometers is much lower than the repetition frequency of the passively mode-locked fiber lasers, making it impossible to obtain the single-shot time profiles or single-shot spectrums of each RT. The DFT technique provides a method to overcome the limitations of sampling speed and bandwidth of electronic equipment to realize continuous, ultrafast, and shot-to-shot data acquisition.

As shown in figure 1**a**, the DFT technique is based on the analogy between spatial Fraunhofer diffraction and time dispersion, that is, the diffraction of pulses through a lens in the far-field region is equivalent to the pulse transmission in the dispersive element. The typical implementation system of the DFT technique is shown in figure 1**b** where each pulse will be stretched during the transmission due to the large group velocity dispersion (GVD) of the dispersive element, and spectrums will be mapped into time profiles. The stretched pulse is detected and recorded by a high-speed photodetector

Accepted Manuscript

combined with a high-speed real-time oscilloscope. The information recorded by the oscilloscope is then input into the computer for data processing to capture the real-time shot-to-shot spectrum evolution of soliton pulses. As the scanning frequency of the high-speed oscilloscope (up to 10 GHz) can be about ten orders of magnitude higher than commercial spectrometers, the DFT technique can be used to obtain the solitons' single-shot spectrums. In other words, it provides an excellent method for analyzing the dynamic characteristics of soliton pulsations and soliton explosions in passively mode-locked fiber lasers. The basic principle, data acquisition, and data processing of the DFT technique are described below.

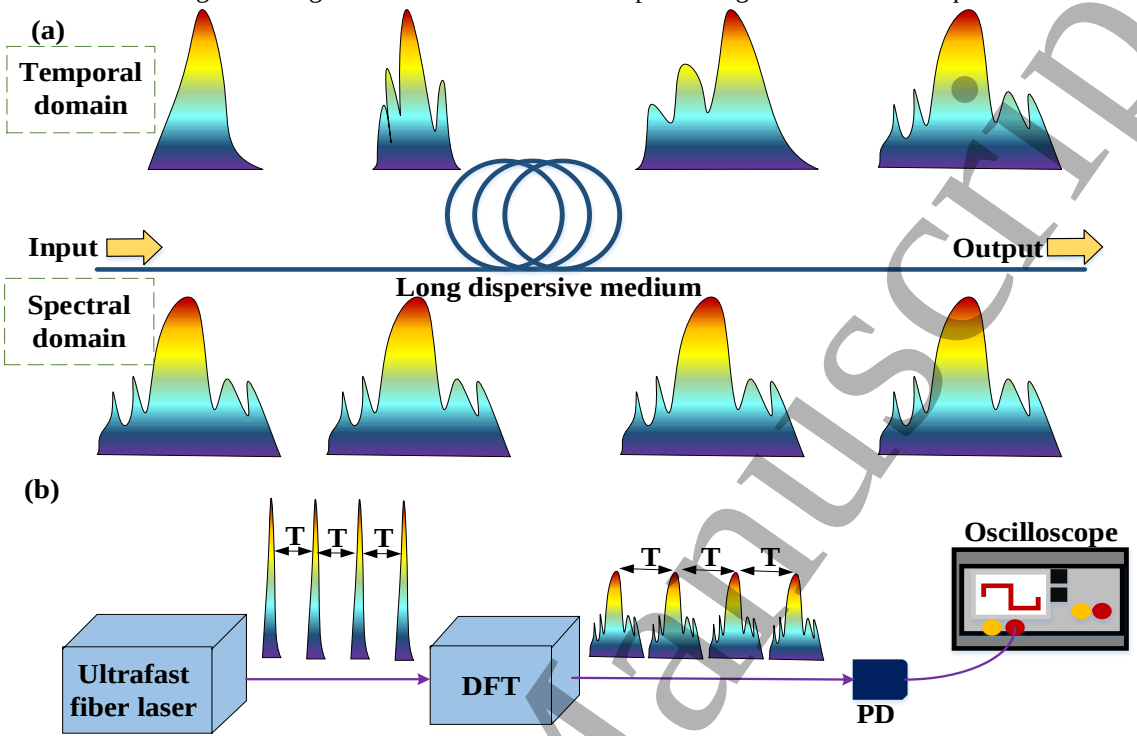


Figure 1. The (a) principle and (b) system of the DFT technique.

2.2.1 Basic principle

In general, the several kilometers of DCF or the longer SMF can be used as the dispersion element of the DFT technique. The incident pulses need to be attenuated appropriately to avoid spectrum distortion induced by the nonlinear effect in the fiber. Because most passively mode-locked fiber lasers use fiber pigtails for output, undoubtedly, using SMF as the dispersive element is unquestionably the most practical option. To illustrate the basic principle of the DFT technique, consider SMF as the dispersive element. Let L and *t* be the length of the fiber and the evolution time, the definitions of other parameters are the same as in Table 1. When only considering the β_2, ignoring fiber nonlinear effect and loss, the response function can be expressed as:

$$H(\omega - \omega_0) = \exp[\frac{-i(\omega - \omega_0)^2}{2}\beta_2 L] \quad (23)$$

According to the nature of the Fourier transform, its corresponding function in the time domain is given in equation (24):

$$h(T) = \exp[i\frac{T^2}{2\beta_2 L}] \quad (24)$$

The output for the input pulse $U(0, T)$ can be represented by equation (25):

$$U(L,T) = U(0,T) * h(T) = \int_{-\infty}^{+\infty} U(0,T')\exp[i\frac{(T - T')^2}{2\beta_2 L}]dT' \quad (25)$$

where * represents convolution, and T' is time. If the detected signal is distributed in the time-bandwidth of ΔT_0 and meets the condition of $\frac{\Delta T_0^2}{2\beta_2 L} \ll 1$, equation (25) can be approximated as:

$$\exp[i\frac{T^2}{2\beta_2 L}]\int_{-\infty}^{+\infty} U(0,T')\exp[i\frac{TT'}{\beta_2 L}]dT' \quad (26)$$

According to the definition of Fourier transform, the output is:

$$U(L,T) = \exp[i\frac{T^2}{2\beta_2 L}]\tilde{U}(0,\omega)\Big|_{\omega=\frac{T}{\beta_2 L}} \quad (27)$$

$\tilde{U}(0,\omega)$ represents the Fourier transform of $U(0,T)$. It can be seen from equation (27) that after stretching, the information of soliton spectrums is mapped to its time profiles.

2.2.2 Data collection

Accepted Manuscript

The time train corresponding to the spectrum of the stretched soliton pulses can be obtained by the high-speed photodetector and the high-speed digital oscilloscope. The conversion relationship between the time coordinate and the wavelength is:

$$\lambda - \lambda_A = \frac{T - T_A}{|D|L} \tag{28}$$

$D = -2\pi c\beta_2 / \lambda^2$, c and λ represent the fiber dispersion parameter, the speed of light in the vacuum, and the pulse wavelength, respectively. λ_A and T_A are the characteristic wavelengths of the spectrum and their corresponding delay. As T_A cannot be derived directly from the experiments, it is usually necessary to find some characteristic wavelengths such as the position of Kelly sidebands to convert the time information into the spectrum through the equation (28). The spectral resolution is determined by the sampling rate (f_{sam}) of the analog-to-digital converter, the detection bandwidth (f_{det}), and the far-field spectral resolution (f_{GVD}) which is related to the GVD [54-56]. The final spectral resolution is the maximum of the above values:

$$\delta\lambda = max(\delta\lambda_{max} = \frac{1}{f_{sam}|D|L}, \delta\lambda_{det} = \frac{0.35}{f_{det}|D|L}, \delta\lambda_{GVD} = \lambda_0\sqrt{\frac{2}{c|D|L}}) \tag{29}$$

It can be seen from the equation (29) that increasing the total dispersion value $|D|L$ is beneficial to distinguish the detailed information of spectrums, but is limited by the expandable width. By passing through the dispersive element, the expanded time width of pulses can be expressed as $T_\omega = |D|L\Delta\lambda$, where $\Delta\lambda$ is the spectral width of the dissipative structure under test. To avoid the overlapping of pulses in two adjacent RTs, it is necessary to ensure that T_ω is smaller than the RT time. To obtain the spectrum of each pulse, it is crucial to carefully determine the value of $|D|L$ to prevent overlapping of the spectrum, especially when there are separate multi-pulses in one RT.

There is a certain contradiction between the spectral resolution and detection sensitivity of the DFT technique. On the one hand, faster detection means shorter integration time and fewer photons collected. This reduces the sensitivity of the photoelectric detection system. On the other hand, increasing the total dispersion value $|D|L$ improves the resolution of the system, but at the same time increases the system loss and reduces the number of photons per unit of time, which reduces the sensitivity. The aperture error caused by the quantization noise of analog-to-digital converters and the jitter of the sampling clock will also adversely affect the test accuracy and sensitivity [57]. Low sensitivity may result in the microstructured spectrums or weak soliton spectrums submerged in the background noise, necessitating a compromise between resolution and sensitivity is required. Fiber amplifiers can be employed to amplify the stretching or stretched soliton pulses if necessary [54], however, the spectrum distortion induced by the unbalanced gain should be avoided. The fiber Raman amplifier can be constructed by adding pumping sources in the two segments of the fiber because the length of the fiber used as the dispersive element in the DFT technique is normally in the order of kilometers. Then, the distributed Raman amplification effect can be employed to concurrently accomplish the pulse amplification and time stretch simultaneously.

2.2.3 Data processing

The digital time train captured by the oscilloscope must be transferred to the computer for additional processing. To begin, the time train is segmented based on the RT of the laser to create a two-dimensional space-time diagram. The time coordinate is then converted into frequency or wavelength using the equation (28) to obtain the single-shot spectrum based on the fiber dispersion value and the basic properties of the spectrum. The intensity of the single frame time train is expressed as $|U(L,T)|^2 \propto \tilde{U}(0,\frac{T}{\beta_2 L})\tilde{U}^*(0,\frac{T}{\beta_2 L})$, where $\tilde{U}^*$ is the conjugated of $\tilde{U}$, the discrete Fourier transform is applied on the intensity again, and the spectral information is remapped to the time domain to produce single-shot autocorrelation traces of the measured solitons [58]. Suppose that the number of sampling points for discrete Fourier transform is N, the obtained interval between two discrete points on the autocorrelation traces is

$$\Delta\tau = 2\pi\frac{\beta_2 L f_{sam}}{N} \tag{30}$$

A single-shot autocorrelation trace is a powerful tool for investigating the interaction between solitons. The single-shot autocorrelation trace can be used to retrieve not only the position information between solitons but also the phase change between solitons when there are interference fringes created by multi-solitons in the single-shot spectrum through the DFT technique. By the DFT technique, single solitons, tight solitons molecules, and Kelly sideband (related to the dispersive waves) on the spectrum can be observed, but DC or quasi-DC Q-switched pulses do not have localized features on the time domain, so their spectrum components cannot be reflected in a single-shot spectrum. Combining the DFT technique with the time-lens technique, researchers can simultaneously obtain real-time spectrums and time profiles of the solitons to realize the synchronous characterization of pulse intensity and pulse phase [59]. In addition, the far-field assumption may not be satisfied for some solitons with wide time domain intervals, and the time domain profile and spectrum acquired at this time may not match. The resultant time sequence can be regarded as the coherent superposition

Accepted Manuscript

of each soliton spectrum for the loose bound soliton that is formed of a large number of soliton pulses [60]:

$$|U(L,T)|^2 \propto \left|\sum_{K=1}^{N_S} \tilde{A}_k\left(0,\frac{T-\tau_k}{\beta_2 L}\right)\exp(-i\varphi_k)\right|^2 \quad (31)$$

N_s is the soliton number, A_k, τ_k, and φ_k represent the complex amplitude, position, and phase of each soliton, and k is the serial number. Although the time profile retained after stretching may not directly correlate to the spectrum, the interference fringes can nevertheless convey information about the position and phase disturbances between the solitons, as shown in equation (31). Therefore, the single-shot spectrums information of loosely bound solitons can also be displayed on the high-speed oscilloscope through the DFT technique.

3. Soliton pulsations

3.1 Theoretical research on soliton pulsations

3.1.1 Numerical simulation based on cubic-quintic Ginzberg-landau equation

Period bifurcation occurs when a small change in a system parameter causes the system state to be repeated at multiples of the original system period in nonlinear systems [38]. To duplicate the original state, the system must repeat the integer multiple of the initial cycle iterations. Period bifurcation is a common path to chaos in physics research [61].

CQGLEs can be used to describe the soliton propagation in passively mode-locked fiber lasers [62]. It has different types of solutions including plain pulsating soliton solutions, erupting soliton solutions, and creeping soliton solutions [36, 37]. And all of them show period bifurcation characteristics similar to those in figure 2**a**, belonging to the general chaotic behaviors and the path toward chaos [34, 63, 64]. Figure 2**b** and figure 2**c** show that pulsating soliton solutions have common characteristics, they are periodically repeated along the propagation direction. Figure 2**d** and figure 2**e** show a typical vertical view of the soliton time domain evolution and soliton frequency domain evolution generated through numerical simulations, demonstrating the periodic change of soliton characteristics and pulse energy (figure 2**f**) [65]. Soliton pulsation is the name given to such soliton solutions with periodic evolution features.

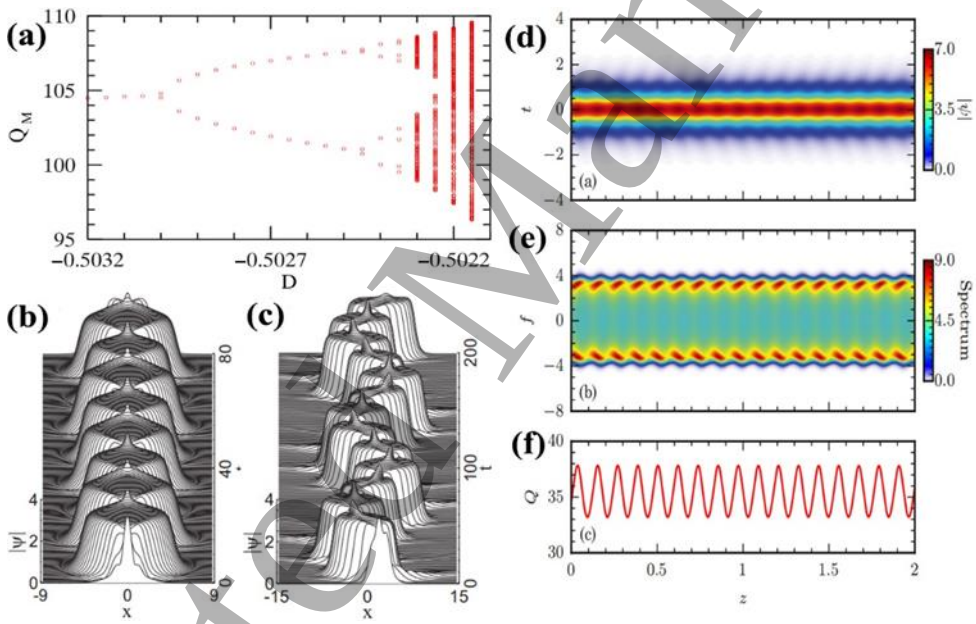


Figure 2. The graphical representation of soliton pulsations. (a) Period bifurcation. Reprinted with permission Ref [36]. Periodical repetition of (b) plain pulsating solitons and (c) creeping pulsating solitons in the propagation direction. Reprinted with permission Ref [64]. Vertical view of (d) time domain evolution, (e) frequency domain evolution, and (f) energy variation of soliton pulsations. Reprinted with permission Ref [36].

Even though numerical simulations have demonstrated the existence of pulsating solutions and their period bifurcations, the search for analytical expressions of pulsating solutions and bifurcation boundaries has been elusive. The moment method [66-68], the Lagrange equation [69], or the variational method [67, 70, 71] can be used to reduce the infinite-dimensional CQGLEs to the five-dimensional model, then the nonlinear part is solved by the RK4IP method and the linear part is solving in Fourier domain [36, 66, 72, 73], which implements the modeling of passively mode-locked fiber lasers. Researchers uncovered that all soliton solutions of CQGLEs had regular evolution patterns of amplitude, frequency, position, width, and chirp [70]. The investigation of various pulsating characteristics induced by the

Accepted Manuscript

combination of two dissipative solitons can be realized by introducing the random component of GVD and employing the variational approximation [74]. The TOD has been proven to eliminate the periodicity of soliton pulsations and transform them into stationary solitons [75]. The mutual transformation between stationary solitons and soliton pulsations may be realized by changing higher-order effects such as IRS, SS, and TOD [67, 69], and the former two effects (IRS, SS) have a stronger influence on soliton pulsations than the third one (TOD) [66]. In the presence of linear gain, nonlinear gain, gain saturation effect, spectral filtering effect, and IRS, the self-frequency shift of stationary solitons and soliton pulsations can be completely suppressed [73]. Moreover, the extreme dissipative soliton pulsations were observed with the change of quintic nonlinear gain coefficient [36], demonstrating that the intra-cavity gain saturation effect can affect the character of soliton pulsations [76]. With the increase in linear gain coefficient and gain saturation intensity, single solitons become unstable, resulting in the formation of single-period soliton pulsations, double-period soliton pulsations, and creeping solitons, and pulsating soliton molecules [72].

It has been evident from research studies that Airy pulses with properties of dispersion-free, self-accelerating, and self-healing make it easier to generate soliton pulsations. When Airy pulse pairs are used as the initial pulses in cubic dispersion fiber, it is discovered that the soliton peak amplitude and the corresponding temporal position will vary with the propagation distance, exhibiting weak oscillation behaviors similar to the soliton pulsations [77]. As depicted in figure 3, through the use of Airy pulse pairs with different pulse intervals as the initial pulses of the passively mode-locked fiber laser based on the CQGLEs, the erupting solitons, zigzag creeping solitons, single-period soliton pulsations, and double-period soliton pulsations can be observed [78]. The erupting solitons are classified as one kind of soliton explosion [79]. To obtain the Airy pulses in the experiment, a cubic spectral phase must be applied to an incident Gaussian pulse using the pulse shaping technique or propagation in the cubic dispersion fiber [80]. Consequently, two Airy pulses with different initial relative phases and time intervals can be created by passing the Airy pulses through the beam splitter and phase plates of different lengths, to be utilized as the pump source in the experiments [79]. However, this is merely an ideal step, the real experiments are more complex and requires consideration of numerous elements, which is challenging. Numerical research seems to be more effective in this case.

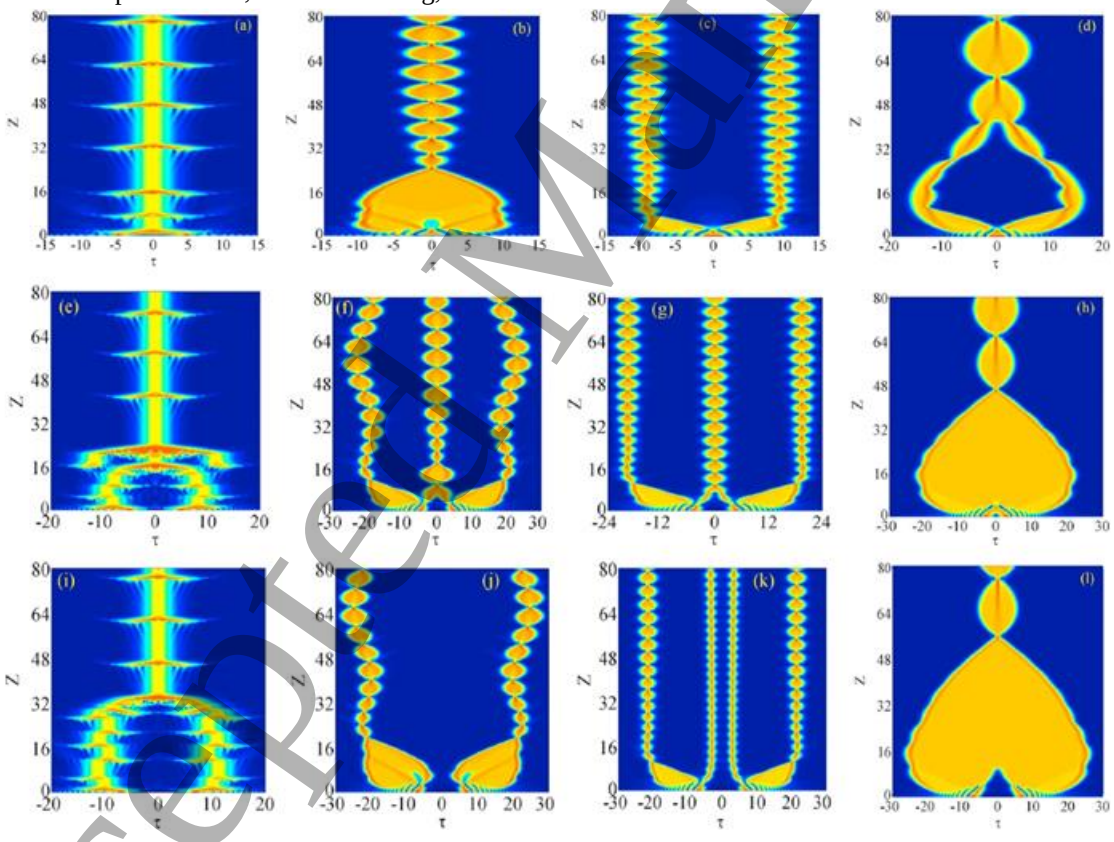


Figure 3. Time evolution of soliton pulsations with different Airy pulse pairs. Reprinted with permission Ref [78].

3.1.2 Numerical simulation based on nonlinear Schrödinger equation and its extend form

The numerical simulation results related to soliton pulsations reported in section 3.1.1 are based on the continuous model, which does not adequately characterize the

Accepted Manuscript

experimental system. By including the pulse propagation period, which is connected to the cavity's RT time, a model that is closer to the actual laser system can be created. This fiber laser modeling technique is known as "parameter management" and it is derived from "dispersion management" in NLSEs with stepwise coefficients in front of the second-order derivative term [81]. This model proved the existence of soliton pulsations with period bifurcations and paved the way to chaos [35, 82]. The lumped model of passively mode-locked fiber lasers based on NLSEs or GLEs is more closer to the actual experimental laser systems [83]. As a result, researchers conducted a related study on soliton pulsations using the lumped model, which will be discussed and examined in this part.

The previous reference reported that as the normalized saturation gain increases, single soliton pulsations and multi-soliton pulsations arise sequentially in the passively mode-locked fiber laser (including long-period fiber grating) based on the complex GLEs [84]. The spectrum of soliton pulsations has two kinds of sidebands under the condition of anomalous dispersion: one is created by the parametric process, and the other is the Kelly sideband [85] which will be broadened during the pulsation process [86]. The existence of soliton pulsation was demonstrated in the numerical simulation of the nonlinear amplifying loop mirror (NALM) passively mode-locked fiber laser based on the NLSEs [87, 88]. And it was determined that the instability of soliton pulsations is related to the reverse-saturation absorption effect of the NALM mode-locker [89]. We discovered that under a fixed output ratio of the coupler with the increase of the small signal gain, there will be various soliton pulsations in the study of the single-walled carbon nanotubes (SWCNTs) passively mode-locked fiber laser based on the GLEs [90]. Especially, we have observed the creeping vibration soliton molecules which also exist in the research of reference [91] and reference [92]. Few research reports found the creeping behavior of pure-quartic soliton pulsations in the NLSEs-based NPR passively mode-locked fiber laser [93]. The redistribution of energy between the center part and the oscillation tail of pure-quartic solitons is responsible for this creeping behavior [94].

Because the NLSEs and GLEs feature a family of soliton solutions termed the Akhmediev breathers, which have properties that are comparable to soliton pulsations in the time domain (as seen in figure 4), soliton pulsation is frequently referred to as the breather [95]. The features of Akhmediev breathers can be affected by the average dispersion and the small signal gain of the passively mode-locked fiber lasers [96]. Researchers successfully manipulated and selected the desired solitons and their evolution dynamics by adjusting the initial relative phase, initial pulse interval, and different soliton order of two different Airy pulses to obtain the single breather, bound breather, and single-parallel breather [97].

Although the NLSEs-based or the GLEs-based passively mode-locked fiber lasers models can better match the actual fiber laser systems, they are dependent on the specific resonator structures and parameters, therefore, the soliton evolution depicted is not universal. The present research is more interested in using the CQGLEs to model passively mode-locked fiber lasers and investigate soliton nonlinear dynamics. The numerical simulation can be used to reveal the relationship between soliton dynamics and laser structural parameters, providing a theoretical foundation for the observation of soliton dynamics in subsequent experiments, and playing a constructive role in the design and development of novel lasers.

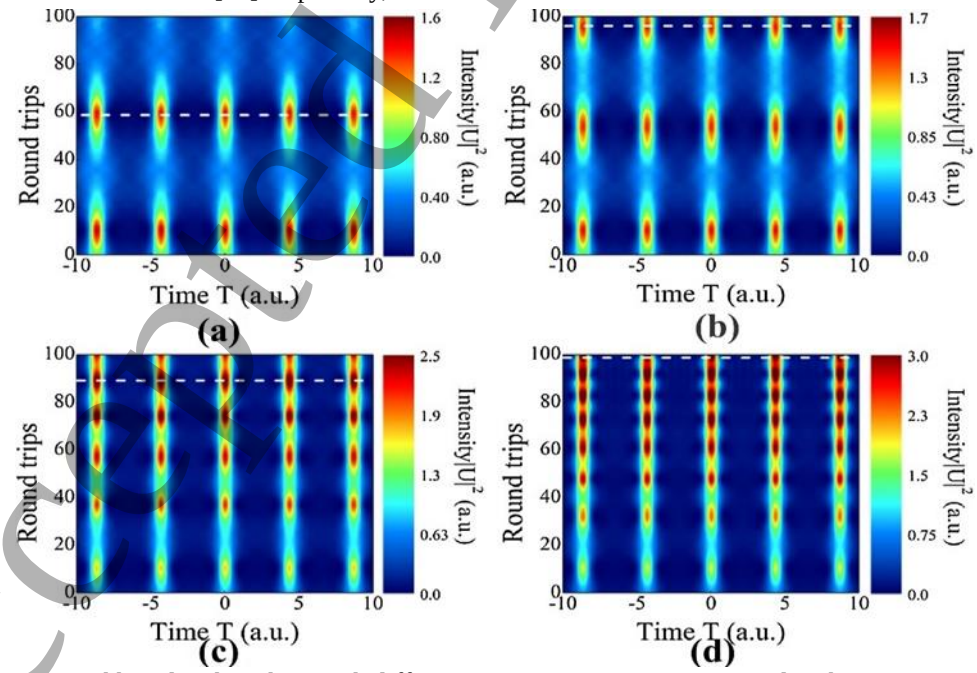


Figure 4. Akhmediev breathers with different system parameters. Reprinted with permission Ref [96].

Accepted Manuscript

3.2 Experimental research on soliton pulsations

3.2.1 Single soliton pulsations

Although soliton pulsations in passively mode-locked fiber lasers have been predicted theoretically for a long time, early experiments could only study soliton pulsations through the periodic change of pulse energy in the oscilloscope track, and the evolution process could not be studied in depth due to detection resolution limits. Scientists have been using the DFT technique to examine the real-time shot-to-shot spectrum evolution of soliton pulsations in nonlinear polarization rotation (NPR) [86, 88, 98-104], NALM [105], nonlinear multimode interference (NL-MMI) [106, 107], SWCNTs [85, 106-115], SnSe [116], graphene [117] passively mode-locked fiber lasers and hybrid mode-locked fiber laser [87, 118] till recently. As shown in figure 5, the pulse shape, width, and amplitude of solitons can be periodically altered by simply adjusting the pump power and the angle of the polarization controllers (PCs). This experiment proved the existence of soliton pulsations and showed that such soliton pulsations are caused by the filtering effect as well as the nonlinear saturated absorption effect. Table 2 lists the parameters of the DFT technique with different elements used in the study of soliton pulsations in section 3.2.

Table 2. Parameters of the DFT technique with different elements in 3.2.

Mode-locked	Gain fiber	Net dispersion	Dispersive medium	Real-time oscilloscope	Photodetector	Spectral resolution	Ref
SWCNT	Er	-0.61 ps^2	15 km SMF	8 GHz	12.5 GHz	0.49 nm	[85]
SWCNT+NPR	Er	--	14 km SMF	18 GHz	--	0.26 nm	[87]
NPR	Er	0.754 ps^2	45 km SMF	--	9.5 GHz	0.38 nm	[98]
NPR	Er	-0.1 ps^2	DCF	8 GHz	12.5 GHz	0.35 nm	[100]
NPR	Er	-0.05 ps^2	14 km SMF	8 GHz	12.5 GHz	0.5 nm	[101]
NPR	Er	0.19 ps^2	45 km SMF	33 GHz	45 GHz	0.152 nm	[102]
NPR	Er	--	SHG	33 GHz	20 GHz	--	[103]
NALM	Yb	--	5 km DCF	33 GHz	25 GHz	0.16 nm	[105]
NL-MMI	Er	0.093 ps^2	10 km SMF	33 GHz	12 GHz	--	[106]
NL-MMI	Er	-0.28 ps^2	15 km SMF	33 GHz	12 GHz	--	[107]
SWCNT	Er	-0.3 ps^2	24 km DCF	33 GHz	15 GHz	0.06 nm	[110]
SWCNT	Er	-0.105 ps^2	--	8 GHz	12.5 GHz	--	[111]
SWCNT	Er	-0.29 ps^2	24 km DCF	33 GHz	15 GHz	0.06 nm	[112]
SWCNT	Er	-0.05 ps^2	5 km DCF	--	--	--	[113]
SWCNT	Er	--	--	33 GHz	50 GHz	0.28 nm	[115]
SnSe	Er	-0.37 ps^2	25 km SMF	12.5 GHz	12.5 GHz	0.18 nm	[116]
Graphene	Er	--	--	36 GHz	50 GHz	--	[117]
NPR+ CNT	Er	--	16 km SMF or DCF	16 GHz	12.5 GHz	0.25 nm or 0.035nm	[118]
NPR	Er	--	11 km SMF	50 GHz	33 GHz	0.025 nm	[119]
NPR	Er	0.24 ps^2	DCF	30 GHz	12.5 GHz	0.22 nm	[120]
NPR	Er	0.19 ps^2	1.5 km DCF	33 GHz	45 GHz	0.152 nm	[121]
SWCNT	Er	-0.96 ps^2	14 km SMF	8 GHz	12.5 GHz	0.43 nm	[122]
NPR	Er	-0.27 ps^2	--	20 GHz	--	--	[123]
NPR	Er	--	11 km DCF	--	50 GHz	0.025 nm	[124]
NPR	Er	-0.37 ps^2	20 km SMF	25 GHz	20 GHz	--	[125]
SWCNT	Er	0.171 ps^2	--	36 GHz	50 GHz	0.15 nm	[126]
NPR	Er	0.19 ps^2	1.5 km DCF	33 GHz	45 GHz	0.152 nm	[127]
NPR	Er	0.02 ps^2	DCF	20 GHz	12 GHz	0.17 nm	[128]

Accepted Manuscript

NPR	Er	--	--	33 GHz	50 GHz	0.025 nm	[129]

In an NPR passively mode-locked fiber laser, we discovered that the change of PCs can affect the breathing characteristic of soliton pulsations [104]. The Lyot filter is an intrinsic birefringence filtering effect produced by the NPR mode-locking technique. Changing the PCs changes the overall intra-cavity birefringence, which modifies the spectrum range and bandwidth of the Lyot filter. As a result, the birefringence filtering effect can impact soliton pulsations, according to our findings. In addition, the self-parametric process [88], the modulation instability [130], the slow gain dynamics [131], and the spectral-filtering-induced instability [98] have also been proved to affect soliton pulsations. Soliton pulsations can be induced by increasing the pump level in the anomalous dispersion region [86] or lowering the pump intensity in the normal dispersion region [98, 119] of passively mode-locked fiber lasers. And the real-time shot-to-shot spectrum evolution has the broadened Kelly sideband [86] or the spike [98] caused by dispersion waves, respectively.

Researchers established that soliton pulsation with Hopf bifurcations is the periodic attractor in dissipative systems and the typical path from stationary to chaos in passively mode-locked fiber lasers through the use of the dispersive temporal holography technique and the DFT technique [38]. As a result, the study of soliton pulsations is frequently linked to chaos. Soliton pulsations can become chaotic in the late stages of energy increase when the spectrum suddenly collapses and then gradually recovers, as it does in soliton explosions [101]. Although such an explosion looks appears chaotic, it possesses periodic characteristics and falls under the soliton pulsations criterion [102]. Especially, invisible soliton pulsations have been found in an NPR passively mode-locked fiber laser through the use of the DFT technique, characterized by solitons that undergo periodic peak power variations but have nearly constant pulse energy [100]. The real-time shot-to-shot spectrum intensity of invisible soliton pulsations at its central wavelength will change periodically due to the effect of self-phase modulation [100]. Coincidentally, SWCNTs passively mode-locked fiber lasers have also been found to have such invisible soliton pulsations [85, 109]. Simultaneously, the double-period soliton pulsations [87, 110], whose pulse intensity changes between two values, were exhibited, as illustrated in figure 5**d-f**, with the solitons' parameter repeats every two oscillations. According to the findings reported in [35], soliton pulsations are tied to a series of periodic bifurcations, and the appropriate selection of cavity parameters can produce any number of pulsating periods. The switching between weak soliton pulsations and extreme soliton pulsations, which are part of the peculiar bicyclic pulsations, remains the coherent state [114]. The existence of a unique type of soliton pulsation called creeping solitons, whose trajectory indicates snake behavior, may be verified using a combination of the time-lens technique and the DFT technique, its corresponding real-time shot-to-shot spectrum evolution depicts breathing characteristics [91].

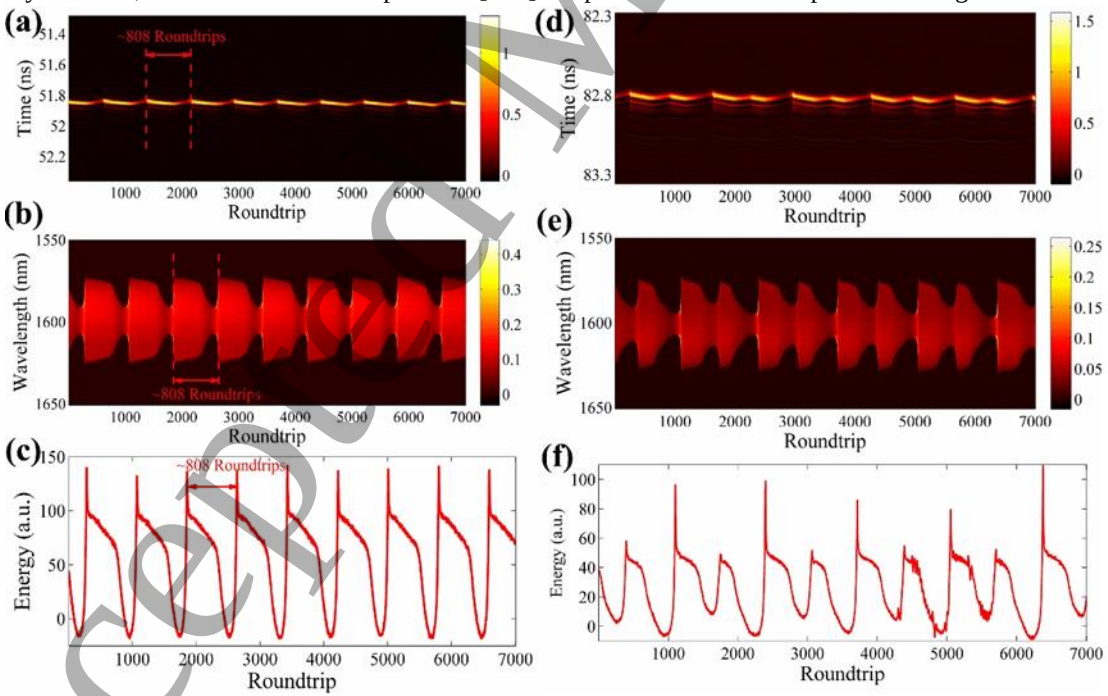


Figure 5. (a)-(c) Single-period and (d)-(f) double-period soliton pulsations: (a)(d) Spatio-temporal dynamics, (b)(e) spatio-spectral dynamics, (c)(f) pulse energy evolution of single-period and double-period soliton pulsations. Reprinted with permission Ref [102].

Accepted Manuscript

The birefringence effect is the key to generating vector solitons in passively mode-locked fiber lasers, it is necessary to utilize polarization-insensitive saturable absorbers such as SWCNTs [113] or NL-MMI [106, 107, 132] to explore the vector characteristics of soliton pulsations. DFT technique can be used to record the real-time shot-to-shot spectrum evolution of vector soliton pulsations to study its transient polarization dynamics. Figure 6**a-i** show that the two orthogonal polarization components have red-shift and blue-shift respectively, and the cross-phase modulation effect can affect such shifts [113]. Reference [106] and reference [107] demonstrated that the two orthogonal polarization components move their center wavelength oppositely to compensate for polarization dispersion. For the transient polarization dynamics of double-period vector soliton pulsations, figure 6**j-m** presents the asynchronous intensity oscillate of the two orthogonal polarization components in the odd and even RTs. Furthermore, the pulse energy evolution of the two orthogonal polarization components in figure 6**no** prove that their pulse energy jumps from the high (low) value to the low (high) value after each RT or has opposite variation [110]. Despite the significant progress noted above, intelligent generation and search of soliton pulsations in passively mode-locked fiber lasers remain difficult since the spectrum and temporal properties of soliton pulsations fluctuate dramatically over the oscillation period. Various soliton pulsation states may be flexibly regulated using an improved depth search algorithm to intelligently change the electronic PCs to produce different modulation depths, resulting in effective searching for soliton pulsations [129, 132, 133].

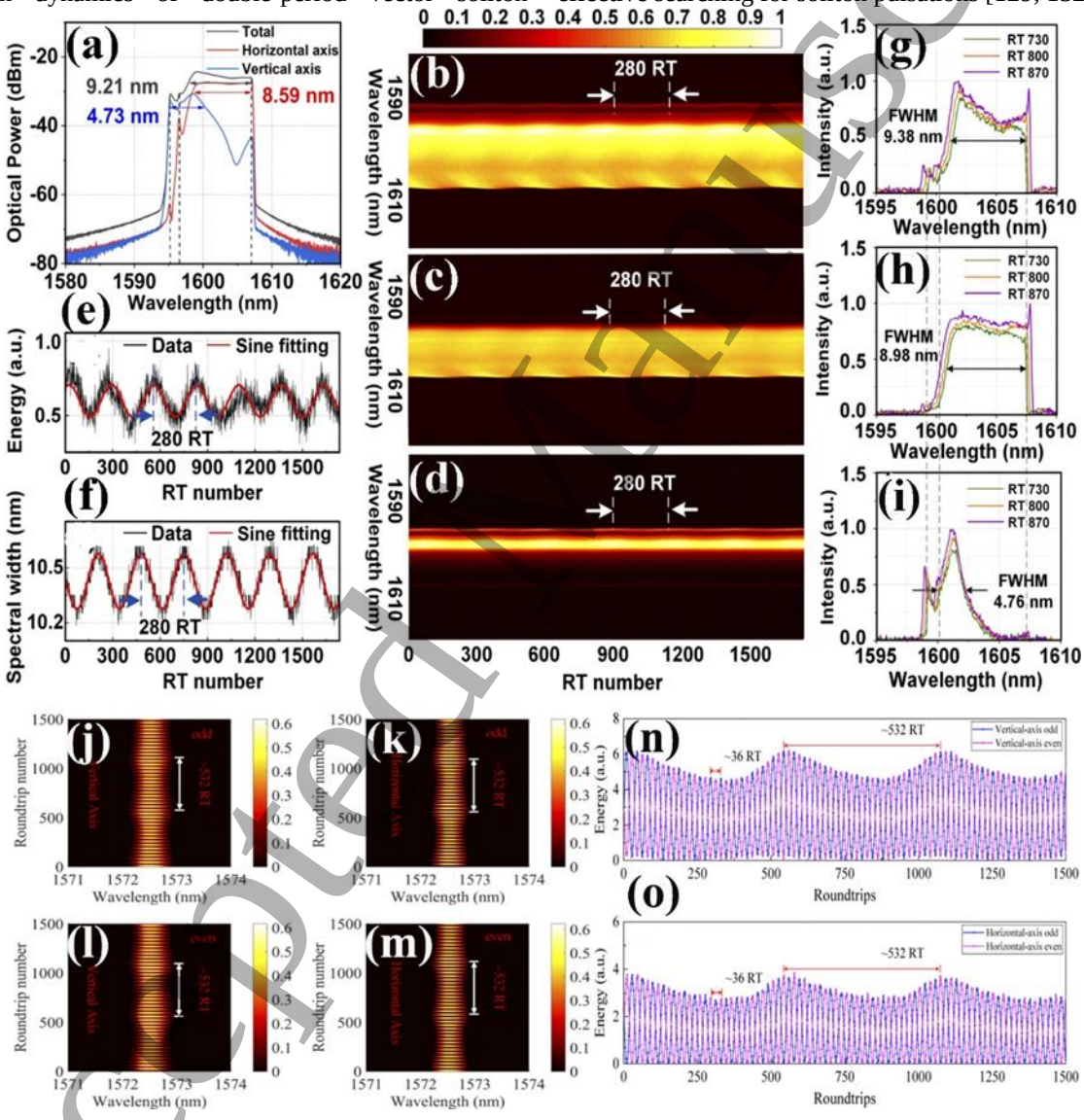


Figure 6. Transient polarization dynamics of vector soliton pulsations: (a) averaged spectrum, (b)-(d) 2D contour plots of the total and the polarization resolved shot-to-shot spectrum, (e)-(f) energy and bandwidth variations versus to RTs, (g)-(i) single-shot spectrum of vector soliton pulsations. Reprinted with permission Ref [106]. Double-period vector soliton

Accepted Manuscript

pulsations: transient polarization dynamics of vector soliton pulsations (j)(k) in the odd RTs, and (l)(m) in the even RTs, pulse-energy evolution of (n) vertical-axis and (o) horizontal-axis. Reprinted with permission Ref [110].

3.2.2 Self-organization of soliton pulsations (multi-soliton pulsations)

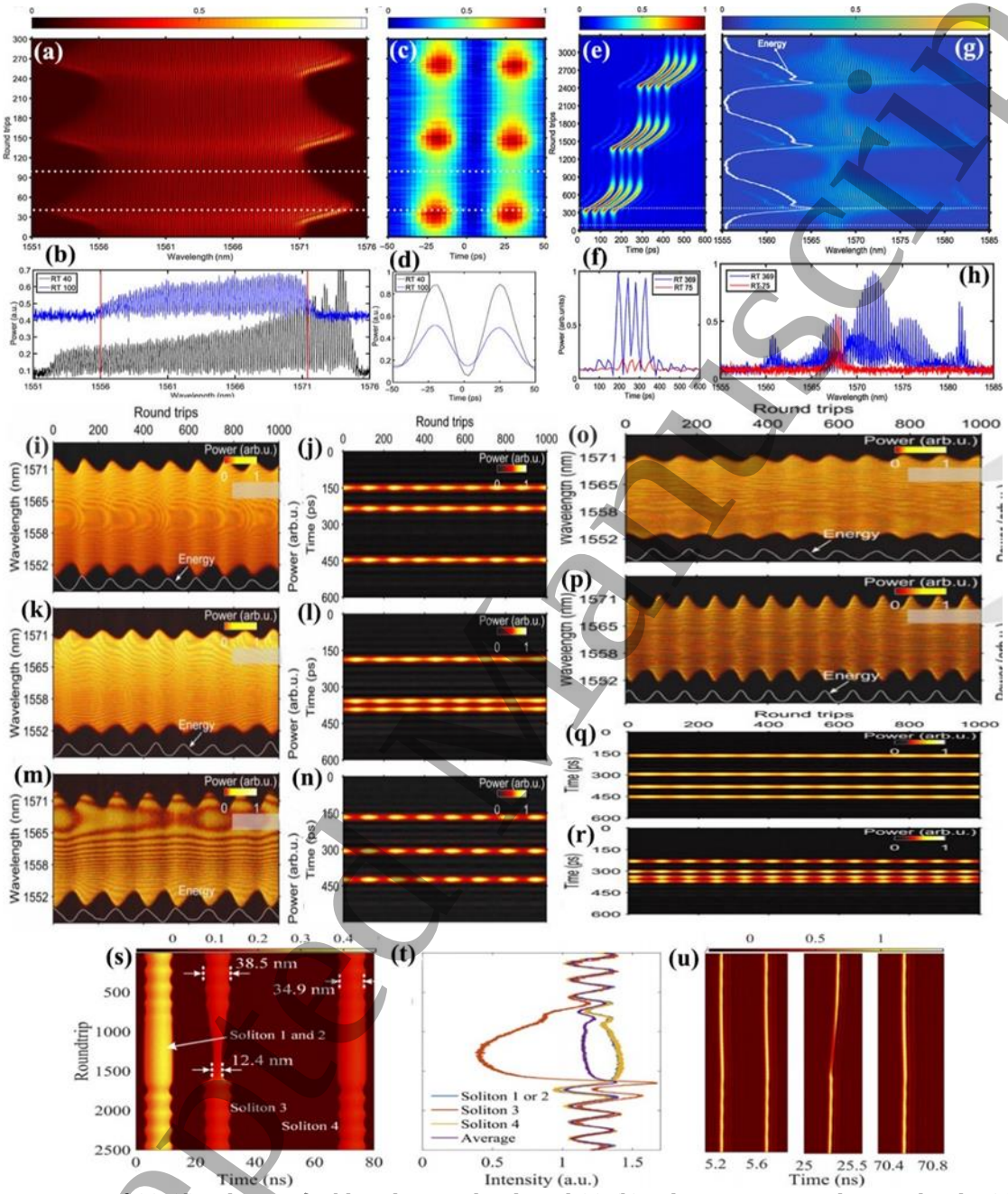


Figure 7. Dynamics of (a)-(d) pulsating double-soliton molecule and (e)-(h) pulsating quartet-soliton molecule: (a)(g) shot-to-shot spectrum evolution recording by DFT technique, (b)(h) single-shot spectrum at the RT numbers of maximal and minimal spectrum in one period, (c)(e) time evolution, (d)(f) time profiles at the RT numbers of maximal and minimal spectrum in one period. Reprinted with permission Ref [119]. Reprinted with permission Ref [134]. Typical evolution of three-soliton pulsating complexes and four-soliton pulsating complexes: shot-to-shot spectrum evolution recording by DFT technique (white curve represents the energy evolution) of (i) (2+1) soliton molecule, (k) (1+2) soliton molecule, (m) three-soliton molecule, (1+3) soliton molecule with (o) large and (p) small internal pulse separations, (j)(l)(n)(q)(r) corresponding

Accepted Manuscript

temporal intensity. Reprinted with permission Ref [129]. Asynchronously evolution of multi-soliton pulsation: (s) shot-to-shot spectrum evolution, (t) energy evolutions, (u) time evolution. Reprinted with permission Ref [121].

As the pumping power of the passively mode-locked fiber lasers exceeds a certain threshold, more than one soliton pulse will appear, and when they are closely spaced because of their interaction, soliton molecules can be formed that exhibit more complex behavior than a single soliton. The autocorrelation trajectory and the soliton spectrum can be used to examine the dynamic features of soliton molecules in five aspects: harmonic order, number of bound solitons, pulse interval, pulse duration, and phase difference. Because the spectrum contains information such as time intervals and relative phases between solitons in soliton molecules, the DFT technique can be used to study the soliton molecule dynamics. For example, researchers have found that the spectrum "breathes" during the build-up and dissociation of stationary soliton molecules [128, 135] or pulsating soliton molecules [103, 105, 121]. They discovered two characteristics of pulsating double-soliton molecules [118, 119, 124], and pulsating quartet-soliton molecules [134]. (1) As shown in figure 7**abgh**, the breathing characteristic of the real-time shot-to-shot spectrum evolution is comparable to that of single soliton pulsations. (2) As shown in figure 7**c-f**, the pulse interval and relative phase difference in the time domain evolution present periodicity oscillate. The solid white line in figure 7**g** shows that the pulse energy of pulsating quartet-soliton molecules periodically evolves with the spectral width and pulse intensity, which is similar to single soliton pulsations. Integrating the spectral density of the entire band yields this energy evolution. The 8th-order harmonic mode-locked soliton molecules with each component can exhibit periodic phase oscillation occurring in the fiber laser by continuously altering the intra-cavity polarization state, which can be viewed as a complex of pulsating soliton molecules [125]. Figure 7**ikm** and figure 7**op** depict shot-to-shot spectrum evolutions of the complex of multi-soliton pulsations that contains different multi-solitons, respectively, which also show breathing behavior. And figure 7**jln** and figure 7**qr** present their corresponding oscillate temporal intensity [129]. One complex multi-soliton that includes one two-soliton molecule and two single solitons, can exhibit asynchronous pulsating as shown in figure 7**s-u** [121].

There are generally only brief interactions and collisions between multi-solitons when the distance between solitons is too vast to create soliton molecules. The DFT technique can be employed to investigate the real-time shot-to-shot spectrum evolution characteristic of multi-soliton pulsations. Through the acoustoptic effect, a large number of solitons are merged into a composite structure of uniformly spaced pulsating soliton clusters in the anomalous dispersion passively mode-locked fiber lasers [117, 123]. The real-time shot-to-shot spectrum evolution obtained using the DFT technique demonstrates that during the soliton pulsations, a spectrum with an obvious Kelly sideband will periodically appear, proving that the dispersive wave plays an essential part in the multi-soliton pulsations [117]. Real-time spectrum characterization of multi-soliton complexes in a normal dispersion passively mode-locked fiber laser recorded by the DFT technique revealed the existence of multi-soliton complexes containing nine distinct single-soliton pulsations [113]. Each soliton might evolve periodically in a different way and present the typical characteristic of soliton pulsations in a multi-solitons complex containing one pulsating three-soliton molecule and one pulsating single-soliton [127]. These findings contribute to a better understanding of the dynamics of multi-soliton passively mode-locked fiber lasers.

4. Soliton explosions

4.1 Theoretical research on soliton explosions

4.1.1 Numerical simulation based on cubic-quintic Ginzberg-landau equation

The CQGLE is an amplitude equation describing the onset of Andronov-Hopf bifurcations in dynamical systems and is widely used to analyze the pulse evolution in passively mode-locked fiber lasers [136]. CQGLEs exist for a family of soliton solutions known as soliton explosions whose initial spectrum bursts into several fragments and eventually reverts to the prior state within specified RTs (as illustrated in figure 8**b**) [137-139]. The explosion and self-recovery behavior of solitons are related to Shilnikov's theorem [140]. Figure 8**a** depicts the time evolution of the soliton explosions with the time shift, which is also the characteristic of soliton explosions. It is demonstrated that the quintic nonlinear γ, parameter k, and bifurcation function μ play a key role in the control of soliton explosions using the modified Jacobian elliptic function method [141]. By changing the value of the bifurcation function μ, researchers obtained the soliton explosions with different period bifurcation diagrams, indicating that explosion occurs near the boundary of the unstable state, therefore, it can be regarded as a path from stationary to chaos [142-145]. Figure 8**c** proved that period-halving bifurcations lead to orderly (periodic) explosions, figure 8**d** presented that period-doubling bifurcations lead to chaos [145]. A more complex hidden Markov model can be used to better understand the dynamics of soliton explosions, and it has been discovered that there is a particular range of bifurcation functions where asymmetric soliton explosions produce the successive time shift in their time evolution [141]. Even though the spectrum changes during each period of

Accepted Manuscript

asymmetric soliton explosions are not the same, the time evolution diagram shows a similar time shift.

Soliton explosions can be induced under the influence of additive noise or multiplicative noise over a wide range of bifurcation function values [146, 147]. Many other behaviors, such as exploding, collapsing, filling, and space-time chaos, occurred as a result of the ratio between additive and multiplicative noise intensities [148]. Adding noise widens and concentrates the time distribution between soliton explosions in a shorter time, and the average time between soliton explosions obeys the power law [149]. Researchers established that the number of soliton explosions increases with the growth of fiber dispersion value and that a higher nonlinear gain value can inhibit the occurrence of soliton explosions by introducing a section of anomalous dispersion fiber to realize the model of the dispersion management passively mode-locked fiber laser [150]. Within the framework of coupled CQGLEs for back-propagating waves, it was proved that the collision between two back-propagating dissipative solitons induced the bound soliton explosions and the complex of soliton explosions [151].

Periodic soliton explosion occurs when higher-order nonlinearities (self-frequency shift, SS, IRS) and TOD are added to the CQGLEs to model passively mode-locked fiber lasers [147, 153]. Only complex CQGLEs have periodic soliton explosions with a triangular temporal distribution between each explosion [152]. Periodicity of soliton explosions can be eliminated by appropriately conjugated self-frequency shift, SS, and TOD two by two [153, 154]. Furthermore, the interaction of higher-order terms impacts the splitting modes of the periodic soliton explosions, allowing for controllable selection of right or left periodic explosions [136, 145]. In addition, the soliton explosions can be controlled by the intra-cavity nonlinear phase shift, dispersion, higher-order effects, and soliton interactions, according to the numerical simulation results. The soliton explosions dynamics are theoretically predicted in the continuous model, however, the actual passively mode-locked fiber laser systems are not continuous. To study the soliton explosions, a theoretical model that is closer to the actual lasers must be established.

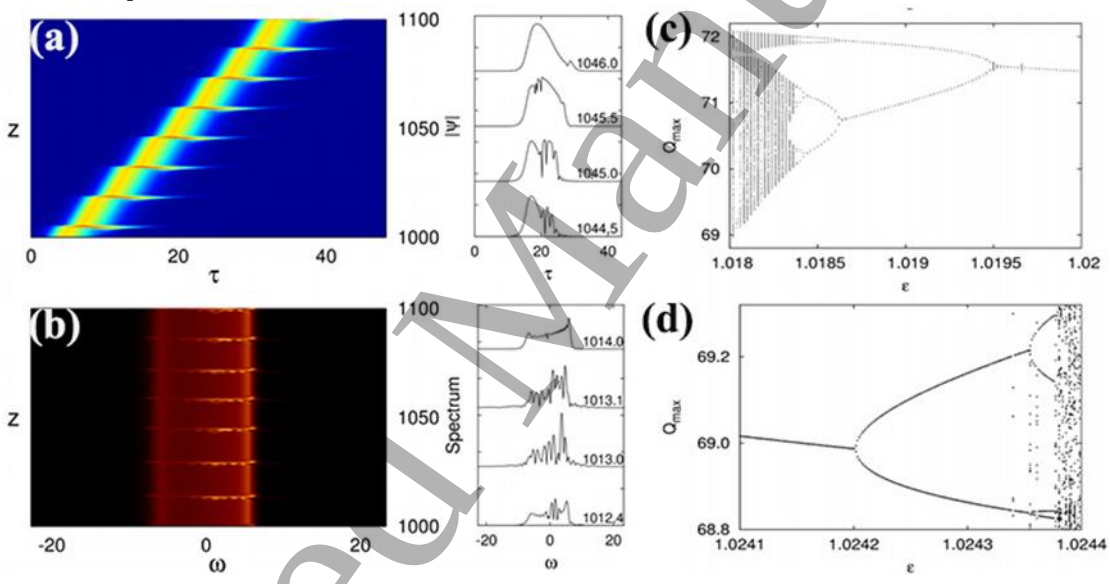


Figure 8. (a) Time evolution and (b) spectrum evolution of symmetric periodic soliton explosions, (c) period-halving bifurcations lead to order, (d) period-doubling bifurcations lead to chaos. Reprinted with permission Ref [145].

4.1.2 Numerical simulation based on nonlinear Schrödinger equation and its extended form

In addition to the CQGLE-based continuous model of passively mode-locked fiber lasers, the lumped model based on the NLSEs or the GLEs can also be used to numerically simulate the characteristic of soliton explosions in passively mode-locked fiber lasers, in which the effect of each cavity component on soliton pulses must be considered. The effect of all parameters in the lumped model of a NALM passively mode-locked fiber laser on soliton pulses was explored, and soliton explosions were proven to exist [155]. By continually modifying the pump power and introducing the band-pass filter into the lumped model of the passively mode-locked fiber lasers, asymmetric soliton explosions occur in the cavity [156-160]. Because the initial pulses and the model itself are both symmetrical, indicating that asymmetric soliton explosions are the default mode of the passively mode-locked fiber lasers [156]. During the process of asymmetric soliton explosions, dark solitons (DAS) can coexist alongside bright solitons [160]. The time domain evolution diagram and spectrum evolution diagram of asymmetric soliton explosion are shown in figure 9. Transient soliton molecules emerge in the process of soliton explosions, which belongs to the special

Accepted Manuscript

soliton explosions, that is, dual pulse instability. Through the spectral filtering effect, the double pulse instability can be turned into the typical soliton explosions, and the multi-solitons by reducing the concentration loss under specific parameters [159]. Soliton explosions may not be desired for usage in passively mode-locked fiber laser systems because they induce time jitter, intensity variation, and spectrum burst. Numerical simulation can help with the design of ultrafast passively mode-locked fiber lasers as well as provide insight into the nonlinear dynamics of ultrafast dissipation systems.

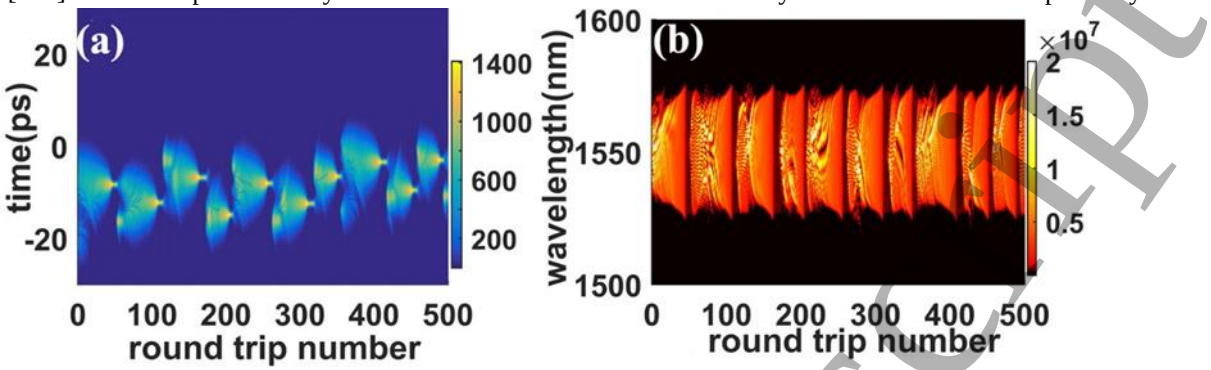


Figure 9. (a) Time evolution and (b) spectral evolution of asymmetric soliton explosions. Reprinted with permission Ref [159].

4.2 Experimental research on soliton explosions

4.2.1 Typical soliton explosions

In 2002, Nail Akhmediev et al. firstly observed soliton explosions in the Ti:sapphire mode-locked laser [161]. However, due to the limitation of testing methods, it is difficult to conduct some in-depth research on soliton explosions characteristic in passively mode-locked fiber lasers in the early years. Recently, the detailed real-time shot-to-shot spectrum evolution of soliton explosions can be recorded using the DFT technique, which is of great significance for analyzing the characteristic of soliton explosions [162]. Table 3 lists parameters of the DFT technique with different elements used in the study of soliton explosions in section 4.2.

Table 3. Parameters of the DFT technique with different elements in 4.2.

Mode-locking	Gain fiber	Net dispersion	Dispersive medium	Real-time oscilloscope	Photodetector	Spectral resolution	Ref.
SWCNT	Er	0.171 ps^2	0.5 km DCF	12.5 GHz	50 GHz	0.2 nm	[106]
NPR	Er	-0.087 ps^2	15 km SMF	16 GHz	12.5 GHz	0.31 nm	[163]
SESAM	Er	--	6.354 km DCF	6 GHz	12 and 45 GHz	0.24 nm	[167]
NPR	Er	--	DCF	20 GHz	32 GHz	0.17 nm	[168]
NPR	Yb	--	12 km SMF	2 GHz	12.5 GHz	--	[170]
NALM	Yb	--	10 km NDF	2.5 GHz	5 GHz	--	[171]
SESAM	Yb	--	15 km SMF	8 GHz	12.5 GHz	0.29 nm	[172]
NPR	Er	--	11 km SMF	33 GHz	50 GHz	0.025 nm	[173]
NALM	Yb	--	10 km NDF	--	30 GHz	0.1 nm	[174]
NPR	Er	--	11 km SMF	33 GHz	50 GHz	--	[175]
NALM	Yb	--	10 km SMF	12.5 GHz	12 GHz	0.2 nm	[176]
SWCNT	Er	--	14 km SMF	8 GHz	12.5 GHz	--	[177]
SWCNT	Er	--	14 km SMF	8 GHz	12.5 GHz	--	[178]
SWCNT	Er	0.171 ps^2	DCF	20 GHz	12 GHz	0.17 nm	[179]
SWCNT	Er	0.13 ps^2	DCF	20 GHz	12 GHz	0.17 nm	[180]

Accepted Manuscript

With the help of the DFT technique, it is reported that the increase in pump power results in the occurrence of soliton explosions between stable mode-locked and noise-like pulses of passively mode-locked fiber lasers [106, 163-170]. Figure 10**b-g** depicts the real-time shot-to-shot spectrum evolution of solitons. As can be observed, the soliton spectrum splits into several fragments before reverting to its original spectrum, which is the typical characteristic of solitons in simulation studies. Figure 10**ai** confirms the time shift in the soliton explosions' time evolution in simulation research, which is attributed to the change of v_g, the combination of transient central wavelength shift, and the change of nonlinear refractive index during soliton explosions [163]. The typical soliton explosions turn into huge soliton explosions (solitons explode one by one) by raising the pump power and slightly adjusting the blade orientation of PCs [165]. The polarization distribution of dissipative soliton explosions was studied using a polarization-state analyzer to detect the soliton spectrum at various pump powers. It was evidenced that during dissipative soliton explosions, the phase diagram had more frequencies with extreme or abnormal polarization state fluctuations [106]. The association between the spectrum collapse of vector soliton explosions and the development of red-shift is presented in experiments on the vector dynamics of incoherent dissipative solitons in ultrafast passively mode-locked fiber lasers [167]. As shown in figure 10**h**, the x-direction spectrum collapses at 3390 RTs, resulting in a red-shift of about 20 nm from the central wavelength of the corresponding y-direction spectrum. In 2018, studies reported that the mutually ignited explosions in a multi-soliton fiber laser, that is, soliton can cause the explosion of another soliton through the soliton interaction mediated by the transient gain response of intra-cavity gain fiber (Er-doped fiber) [168].

The solid green line in Figure 10**b** presents that the pulse energy of soliton explosions will increase significantly as an explosion occurs, creating a powerful condition for the formation of optical rogue waves (ORWs) with high amplitude [178]. Real-time shot-to-shot spectrum evolution of soliton explosions recorded by the DFT technique shows that there are few large fluctuations in the event of Raman Stokes sideband explosions, evidencing the existence of optical rogue waves [171]. Some reports also prove that the collision of breathing solitons will significantly enhance the amplitude of optical rogue waves in bidirectional SWCNTs passively mode-locked fiber lasers [179, 180]. Soliton explosions with a period of hundreds of RT times can provide more opportunities for the appearance of optical rogue waves [171, 179]. Tuning the period of soliton explosions can be achieved by adjusting the PCs and birefringence filter effect [169], it can last for thousands of RT times [170]. Researchers used mutual information to investigate soliton explosions in passively mode-locked fiber lasers and discovered that soliton explosions are correlated using both Pearson correlation and mutual information, which helps to comprehend the complexity of laser systems [166]. The above study further proves that soliton explosions are the inherent property of passively mode-locked fiber lasers.

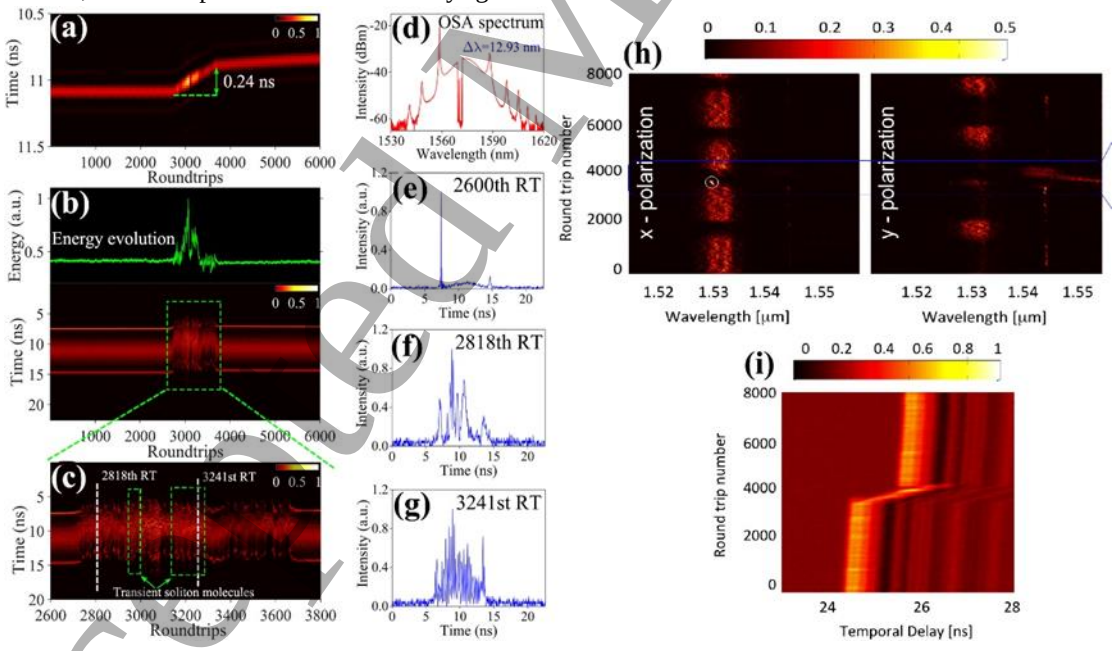


Figure 10. (a) Time domain evolution, (b) shot-to-shot spectrum and corresponding energy evolution, (c) zoom-in spectrum, (d) OSA spectrum, (e)–(g) spectrum at 2600 RT, 2818 RT, and 3241 RT of soliton explosions. Reprinted with permission Ref [163]. (h) Polarization-resolved shot-to-shot spectrum evolution and (i) temporal zoom of the corresponding optical intensity evolution over 8000 RTs of the vector incoherent soliton explosions. Reprinted with permission Ref [167].

Accepted Manuscript

4.2.2 Periodic soliton explosions

Research showed the transition of soliton states from stationary solitons to soliton explosions and then to huge soliton explosions in the SWCNTs passively mode-locked fiber laser by modifying the pump power level in 2016, demonstrating that soliton explosion is related to the intra-cavity nonlinear effect [181]. Similar phenomena can also be observed in NPR mode-locked fiber laser with the increase of pump power, as depicted in figure 11**a-f** [173]. The huge soliton explosions that can behave continuously and periodically from explosion to explosion, called successive soliton explosions, were established using the DFT technique to define the real-time shot-to-shot spectrum evolution of soliton [177]. Figure 11**gh** presents the temporal evolution and the shot-to-shot spectrum evolution of soliton collision-induced soliton explosions [173]. In addition, periodic soliton explosions can be induced by periodic soliton collisions in the semiconductor saturable absorber mirror (SESAM) passively mode-locked fiber laser [172] and the NPR passively mode-locked fiber laser [173]. The periodic soliton explosions that result from the periodic collision of vector solitons are detected in a two-wavelength Tm-doped mode-locked fiber laser with the help of the second harmonic generating technique [182]. The time domain evolution of periodic soliton explosions in figure 11**n** presents the continuous time shift [176], and the real-time shot-to-shot spectrum evolution in figure 11**ijm** shows periodic changes which are extremely similar to the typical soliton pulsations observed in previous publications cited in section 4.2.1. Although the shot-to-shot spectrum change of each explosion in figure 11**ijm** has never been accurately repeated, it can still be called periodic soliton explosions.

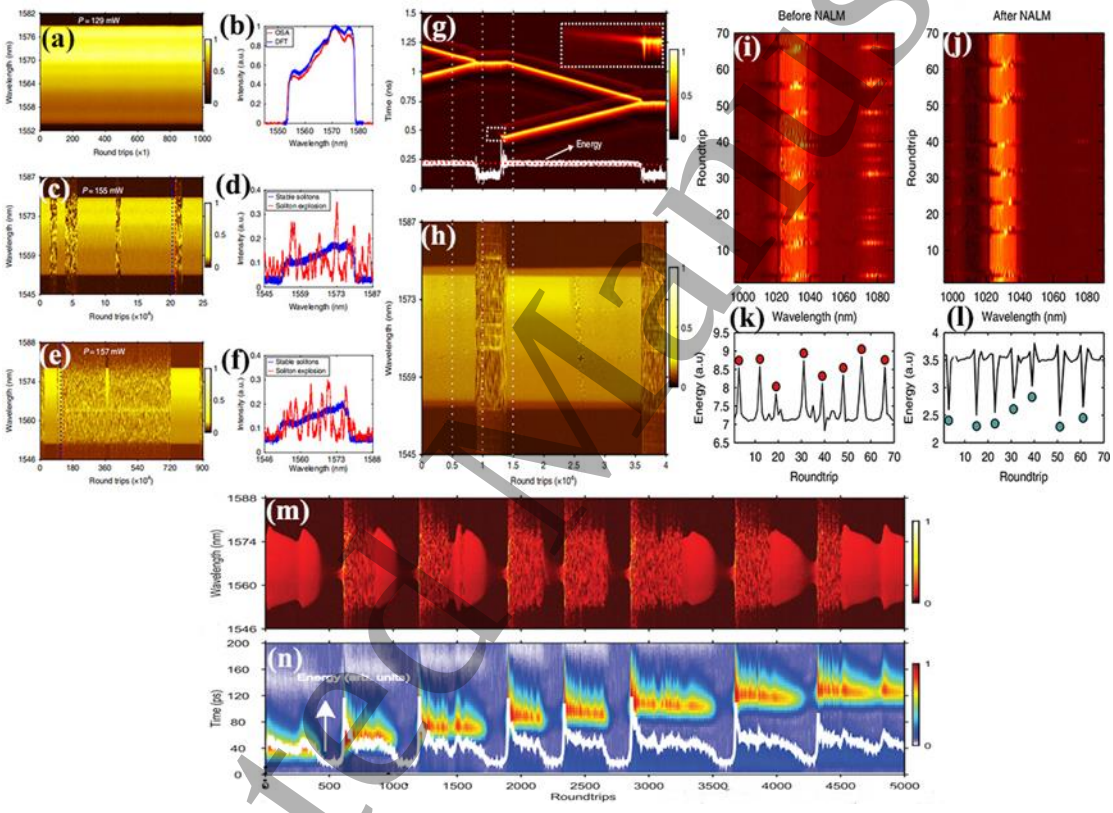


Figure 11. Stable mode-locking, soliton explosions, and soliton collision-induced explosions: (a) shot-to-shot spectrum evolution, (b) single-shot spectrum measured by OSA (red) and DFT (blue) of stationary solitons; (c) shot-to-shot spectrum evolution of soliton explosions under pump power of 155 mW and (e) 157 mW, (d)(f) two cross-sections of stationary solitons and soliton explosions; (g) the spatio-temporal intensity evolution, and (h) shot-to-shot spectrum evolution of soliton collision induced explosions. Reprinted with permission Ref [173]. Shot-to-shot spectrum evolution (i) before and (j) after the NALM mode-locker of periodic soliton explosions, (k)(l) pulse energy of periodic soliton explosions. Reprinted with permission Ref [174]. (m) Shot-to-shot spectrum evolution and (n) time evolution of breathing dissipative soliton explosions. Reprinted with permission Ref [175].

The pulse energy of periodic soliton explosions also increases significantly when the explosion occurs, as seen by the solid white line in Figure 11**n**. However, the energy of each explosion in periodic soliton explosions in NALM

Accepted Manuscript

passively mode-locked fiber lasers is significantly lower than that of separating soliton explosions as illustrated in figure 11**kl** [174, 176], which is inconsistent with the energy increase caused by soliton explosions in previous references [175]. The presence of Raman waves during the periodic soliton explosions may account for this energy reduction [174, 176]. Because the spectrum evolution process of breathing solitons is fundamentally periodic, its explosions process also exhibits periodicity, as demonstrated in figure 11**mn**. The reduced pump power of unidirectional NPR passively mode-locked fiber lasers can cause breathing dissipative soliton explosions [175], whereas, in the bidirectional one, the same explosions can be realized by only changing the polarization settings of PCs [179]. Periodic partial soliton explosions have been found in a NALM passively mode-locked fiber laser by adjusting the position of the output coupler. During the periodic partial soliton explosions, partial strong spectrum interference fringes appear, but a complete collapse of the soliton spectrum is avoided [174]. The accumulated redundant TOD can cause the same phenomenon in the NPR passively mode-locked fiber laser [183]. Indeed, because soliton explosions represent the path to mode-locked instability (chaos), understanding the physics that underpins them gives a useful framework for studying chaotic mode-locked operation over a wider range of experimental parameters.

5. Prospects and summary

To sum up, as efficient paths from stationary to chaos (to achieve chaotic laser output) in passively mode-locked fiber lasers, researchers have extensively investigated soliton pulsations and soliton explosions theoretically by utilizing the continuous model based on the CQGLEs and the lumped model based on the NLSEs as well as its extended form. As shown in figure 12, using the DFT technique, researchers were able to visualize the real-time shot-to-shot spectrum evolution of soliton pulsations and soliton explosions in passively mode-locked fiber lasers to analyze and verify experimentally single-soliton pulsations, multi-soliton pulsations, typical soliton explosions, and periodic soliton explosions. These findings demonstrate that soliton pulsations and soliton explosions are inherent properties of passively mode-locked fiber lasers. However, in comparison to the complicated parameter spaces of the passively mode-locked fiber lasers, the relevant experimental study so far is only a drop in the ocean, and there are still a huge number of unknown or known properties that need to be discovered or investigated in depth. The following are some prospective study directions for soliton pulsations and soliton explosions.

(1) Improvement of the theoretical models: We can understand the fundamental properties of soliton pulsations and soliton explosions by taking into account the detailed description of key components in the simulation using the complex CQGLEs and the NLSEs as well as its extended form. It is necessary to establish a more general model for studying the instability of passively mode-locked fiber lasers. Researchers may define soliton pulsations and soliton explosions with more extensive degrees of freedom and explain the physical mechanism of their production in passively mode-locked fiber lasers by adding the set coordinate to the simulation models [184-187].

(2) The control of the generation of soliton pulsations and soliton explosions: Among the numerous mode-locking techniques, the NPR technique has been widely studied due to its simplicity. However, controlling polarization in the NPR technique is always a challenge, especially obtaining the soliton explosions or soliton pulsations. Self-mode-locking is an effective method for precisely controlling the mode-locking state. It controls the intra-cavity electronic control device using high-speed computing equipment such as a computer central processing unit, single-chip microcomputer, or field programmable gate array to replace the role of the human during the adjustment of mode-locking to achieve the target mode-locked state. Self-mode-locking has been used to regulate the features of soliton pulsations in fiber lasers in the past [118, 133, 175, 188], but there have been no reports on controlling soliton explosions. Self-mode-locking is a promising research avenue for controlling the characteristics of soliton explosions.

(3) Analysis of real-time time characteristics of soliton pulsations and soliton explosions: The DFT technique applied in spectrum measurement removes a bottleneck in research on real-time shot-to-shot spectrum evolution characteristics of soliton pulsations and soliton explosions in passively mode-locked fiber lasers, where time domain measurement is primarily dependent on the high-speed oscilloscope. Researchers recently proposed using the time-lens technique to study the real-time time evolution characteristics of ultrafast nonlinear phenomena [189-194]. It has been applied to the research on the incoherent soliton evolution in optical turbulence [192] and the appearance of random respiration in modulation instability [187]. Using a combination of the DFT technique and the time-lens technique, the real-time spectrum and temporal properties of the soliton build-up process [59, 181] and creeping solitons [91] were obtained. This multi-scale real-time measurement method is helpful to better study soliton pulsations and soliton explosions in passively mode-locked fiber lasers.

(4) Analysis of soliton pulsations and soliton explosions in other bands: The experimental observations so far have mostly concentrated on 1550 nm for soliton pulsations and soliton explosions. The development of mid-infrared ultrafast passively mode-locked fiber lasers is accelerating, spurred driven by potential applications in precision micromachining, and molecular processing [194]. The experimental observation of soliton pulsations in the mid-infrared fiber laser [103] and soliton explosions in a two-wavelength Tm-doped

Accepted Manuscript

fiber laser [182] was achieved using a combination of the second-harmonic generation method and the DFT technique. There is still a long way to go to study soliton pulsations and soliton explosions in other bands by employing real-time measurement techniques like the DFT technique and the time-lens technique.

(5) Analysis of multi-soliton explosions: In the field of soliton explosions, most of the existing theoretical and experimental research focuses on single solitons. The mutual ignition explosions mentioned in the previous study [168] corresponds to multi-soliton explosion. There is a lack of sufficient exploration of the formation mechanism of multi-soliton explosions or their special dynamic characteristics, which requires continuous monitoring. To increase the general understanding of complicated fluctuations in fiber lasers such as soliton pulsations and soliton explosions, mutual information may be employed to examine the correlation of multi-soliton in mode-locked fiber lasers [166].

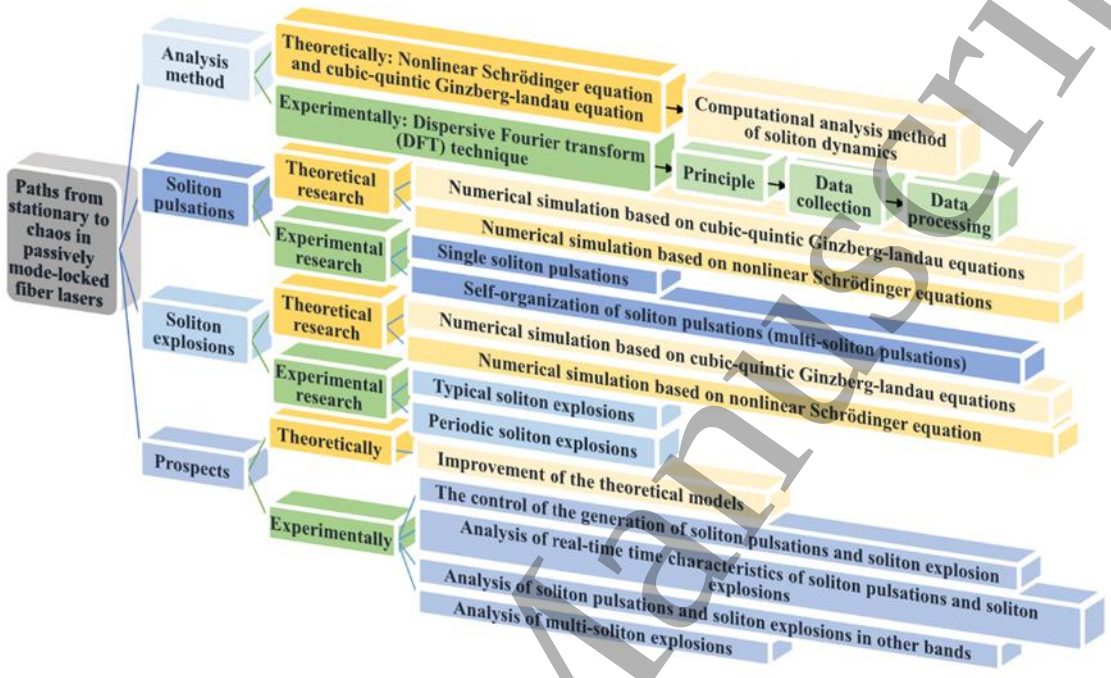


Figure 12. The frame structure of this review.

Acknowledgments

The research was financially supported by the Natural Science Foundation of China (Grant No. 62105209), Jilin Province Science and Technology Development Plan Project (No. 20190201128JC and 20200401125GX), Natural Science Foundation of Guangdong Province (No.2019A1515111060). This project was funded by the Deanship of Scientific Research (DSR) at King Abdulaziz University, Jeddah, under grant no. (KEP-MSc-70-130-42). The authors, therefore, acknowledge with thanks DSR for technical and financial support.

ORCID iDs

Bo Gao: https://orcid.org/0000-0002-8190-7602
Han Zhang: https://orcid.org/0000-0002-0166-1973

Data availability statement

The data that support the findings of this study are available upon reasonable request from the authors.

References

[1] Lorenz E N 1963 *J. Atmos. Sci.* **20** 131-141
[2] Yamada T and Graham R 1980 *Phys. Rev. Lett.* **45** 1322-1324
[3] Locquet A 2020 *Photonics* **7** 1-10
[4] Wang A, Wang Y and He H 2008 *IEEE Photon. Technol. Lett.* **20** 1633-1635
[5] Freire J G and Gallas J A 2010 *Phys. Rev. E* **82** 037202
[6] Simpson T B, Liu J M, Gavrielides A, Kovanis V V and Alsing P M 1995 *Phys. Rev. A* **51** 4181-4185
[7] Abarbanel H, Kennel M, Buhl M and Lewis C 1999 *Phys. Rev. A* **60** 2360-2374
[8] Zhang M and Wang Y 2021 *J. Lightwave Technol.* **39** 3711-3723
[9] FanYi Land JiaMing L 2004 *IEEE J. Quantum. Electron.* **40** 815-820
[10] Annovazzi-Lodi V, Benedetti M, Merlo S, Perez T, Colet P and Mirasso C R 2007 *IEEE Photon. Technol. Lett.* **19** 76-78
[11] Uchida A, Amano K, Inoue M, Hirano K, Naito S, Someya H, Oowada I, Kurashige T, Shiki M,

Accepted Manuscript

Yoshimori S, Yoshimura K and Davis P 2008 *Nat. Photonics* **2** 728-732
[12] Abdullaev F Kh, Gammal A, AM Kamchatnov A M, Tomio L 2005 *Int J Mod Phys B* **19** 3415–3473
[13] Zhang Y P, Wang Z G, Nie Z Q, Li C B, Chen H X, Lu K Q, and Xiao M 2011 *Phys. Rev. Lett* **106** 093904
[14] Wu Z K, Zhang Y Q, Yuan C Z, Wen F, Zheng H B, Zhang Y P and Xiao M 2013 *Phys. Rev. A* **88** 063828
[15] Zhang Z Y, Wang R, Zhang Y Q, Kartashov Y V., Li F, Zhong H, Guan H, Gao K, Li F L, Zhang Y P and Xiao X 2020 *Nat. Commun.* **11** 1-7
[16] Xu C and Wise F 2013 *Nature Photon.* **7** 875–882
[17] Grelu P and Akhmediev N 2012 *Nature Photon.* **6** 84-92
[18] Han Y, Guo Y B, Gao B, Ma C Y, Zhang R H and Zhang H 2020 *Prog. Quantum Electron.* **71** 100264
[19] Ma C, Wang C, Gao B, Adams J, Wu G and Zhang H 2019 *Appl. Phys. Rev.* **6** 041304
[20] Li Y, Gao B, Han Y, Chen B and Huo J 2021 *Frontiers of Physics* **16** 433001
[21] Li X, Feng J, Mao W, Yin F and Jiang J 2020 *J. Mater. Chem. C* **8** 14386-14392
[22] Ma C, Khanolkar A, Zang Y and Chong A 2019 *Photon. Res.* **8** 65-69
[23] Feng T, Li X, Guo P, Zhang Y, Liu J and Zhang H 2020 *Nanophotonics* **9** 2505-2513
[24] Zhao Y, Wang W, Li X, Lu H, Shi Z, Wang Y, Zhang C, Hu J and Shan G 2020 *Acs Photonics* **7** 2440-2447
[25] Xu C and Wise F W 2013 *Nat. Photonics* **7** 875-882
[26] Itoh K, Watanabe W and Ozeki Y 2009 *Proceedings of the IEEE* **97** 1011-1030
[27] Gabel C V 2009 *Contemp. Phys.* **49** 391-411
[28] Nishizawa N 2016 *J. Phys. B: At. Mol. Opt. Phys.* **49** 182003
[29] Kalisky Y and Kalisky O 2011 *Opt. Mater.* **34** 457-460
[30] Kalisky Y and Kalisky O 2010 *Opt. Eng.* **49** 091003
[31] Mihailov S J, Hnatovsky C, Abdukerim N, Walker R B, Lu P, Xu Y, Bao X, Ding H, De Silva M, Coulas D and Grobnic D 2021 *Sensors (Basel)* **21** 1-23
[32] Sciamanna M and Shore K A 2015 *Nat. Photonics* **9** 151-162
[33] Boccaletti S, Grebogi C, Lai Y, Mancini H and Maza D 2000 *Phys. Rep.* **329** 103-197
[34] Akhmediev N, Soto-Crespo J M and Town G 2001 *Phys. Rev. E* **63** 056602
[35] Soto-Crespo J M, Grapinet M, Grelu P and Akhmediev N 2004 *Phys. Rev. E* **70** 066612
[36] Chang W, Soto-Crespo J M, Vouzas P and Akhmediev N 2015 *Phys. Rev. E* **92** 022926
[37] Deissler R J and H. R. Brand 1994 *Phys. Rev. Lett.* **72** 478-481
[38] Wang W, Xian T, Zhang M and Zhan L 2022 *Opt. Lett.* **47** 1234-1237
[39] Wang Y, Wang C, Zhang F, Guo J, Ma C, Huang W, Song Y, Ge Y, Liu J and Zhang H 2020 *Rep. Prog. Phys.* **83** 116401
[40] Chen C J, Wai P K and Menyuk C R 1994 *Opt. Lett.* **19** 198-199
[41] Ma C, Tian X, Gao B and Wu G 2018 *Opt. Commun.* **410** 941-946
[42] Ma C, Tian X, Gao B and Wu G 2018 *Opt. Commun.* **406** 177-182
[43] Bayliss A, Li Y and Morawetz C S 1989 *Math. Comput.* **52** 321-338
[44] Chen B, Jiang T, Zong W, Chen L, Zhang Z and Wang A 2016 *Opt. Express* **24** 16544-16549
[45] Liu S and Wang W 1994 *Phys. Rev. E* **49** 5726-5730
[46] Hirota R 1973 *J. Math. Phys.* **14** 805-809
[47] Nimmo J J C and Crighton D G 1981 *Phys. Lett.* **82A** 211-214
[48] Tang Y and Yan X 2000 *Chinese Phys.* **9** 565-567
[49] Tang Y and Wang W 2000 *Phys. Rev. E* **62** 8842-8845
[50] Chang W, Ankiewicz A, Soto-Crespo J M and Akhmediev N 2008 *Phys. Rev. A* **78** 023830
[51] Anderson D, Lisak M and Reichel T 1988 *Phys. Rev. A* **38** 1618-1620
[52] Anderson D, Lisak M and Berntson A 2001 *Pramana-J Phys.* **57** 917-936
[53] Bale B G, Kutz J N, Chong A, Renninger W H and Wise F W 2008 *J. Opt. Soc. Am.B-Opt. Phy.* **25** 1763-1770
[54] Goda K and Jalali B 2013 *Nat. Photonics* **7** 102-112
[55] Tsia K K, Goda K, Capewell D and Jalali B 2010 *Opt. Express* **18** 10016-10028
[56] Goda K, Solli D R, Tsia K K and Jalali B 2009 *Phys. Rev. A* **80** 043821
[57] Mahjoubfar A, Churkin D V, Barland S, Broderick N, Turitsyn S K and Jalali B 2017 *Nat. Photonics* **11** 341-351
[58] Herink G, Kurtz F, Jalali B, Solli D R and Ropers C 2017 *Sci.* **356** 50-53
[59] Wei X, Li B, Yu Y, Zhang C, Tsia K K and Wong K K Y 2017 *Opt. Express* **25** 29098-29120
[60] Wang Z, Wang Z, Liu Y, He R, Wang G, Yang G and Han S 2017 *Chin. Opt. lett.* **15** 080605
[61] Zhao L, Tang D, Lin F and Zhao B 2004 *Opt. Express* **12** 4573-4578
[62] Ankiewicz A, Akhmediev N and Devine N 2007 *Opt. Fiber Technol.* **13** 91-97
[63] Crasovan L, Malomed B and Mihalache D 2001 *Phys. Lett. A* **289** 59-65
[64] Chang W, Ankiewicz A, Akhmediev N and Soto-Crespo J M 2007 *Phys. Rev. E* **76** 016607
[65] Soto-Crespo J M, Akhmediev N and Ankiewicz A 2000 *Phys. Rev. Lett.* **85** 2937-2940
[66] Uzunov I M, Arabadzhiev T N and Georgiev Z D 2015 *Opt. Fiber Technol.* **24** 15-23

Accepted Manuscript

[67] Uzunov I M, Georgiev Z D and Arabadzhiev T N 2018 *Phys. Rev. E* **97** 052215
[68] Tsoy E N and Akhmediev N 2005 *Phys. Lett. A* **343** 417-422
[69] Latas S C V and Ferreira M F S 2018 *J. Nonlinear Opt. Phys.* **27** 1850008
[70] Mancas S C and Roy Choudhury S 20019 *Chaos Solitons Fractals* **40** 91-105
[71] Ferreira M F S 2018 *IET Optoelectron.* **12** 122-125
[72] He R, Wang Z, Liu Y, Wang Z, Liang H, Han S and He J 2018 *Opt. Express* **26** 33116-33128
[73] Uzunov I M, Arabadzhev T N and Georgiev Z D 2015 *Opt. Quant. Electron.* 47 2969-2981
[74] Parmar G S, Jana S and Malomed B A 2017 *J. Opt. Soc. Am. B* **34** 850-860
[75] Song L, Li L, Li Z and Zhou G 2005 *Opt. Commun*. **249** 301-309
[76] Rozanov N, Fedorov S and Shatsev A 2001 *Optics And Spectroscopy* **91** 232-234
[77] Zhong X, Du X and Cheng K 2015 *Opt. Express* **23** 29467-29475
[78] Zhong X, Liu D, Cheng K and Sheng 2016 *Opt. Commun*. **380** 108-113
[79] Zhong X, Xu J, Wu B and Cheng K 2020 *J. Opt. Soc. Am. B* **37** 645-649
[80] Chang C C, Sardesai H P and Weiner A M 1998 *Opt. Lett.* **23** 283-285
[81] Akhmediev N, Soto-Crespo J, Grapinet M and Grelu P 2005 *J. Nonlinear Opt. Phys.* **14** 177-194
[82] Soto-Crespo J M and Akhmediev N 2005 *Phys. Rev. Lett.* **95** 024101
[83] Han Y, Gao B, Li Y Y, Huo J Y and Guo Y B 2020 *Optik* **223** 165381
[84] Karar A S, Smy T and Steele A L 2008 *IEEE J. Quantum. Electron.* **44** 254-261
[85] Liu M, Wei Z, Li H, Li T, Luo A, Xu W and Luo Z 2020 *Laser Photonics Rev.* **14** 1900317
[86] Du Y, Han M, Cheng P and Shu X 2019 *Opt. Lett.* **44** 4087-4090
[87] Chen J, Zhao X, Li T, Yang J, Liu J and Zheng Z 2020 *Opt. Express* **28** 14127-14133
[88] Peng J and Zeng H 2019 *Phys. Rev. Appl.* **11** 044068
[89] Cai J H, Chen H, Chen S P and Hou J 2017 *Opt. Express* **25** 4414-4428
[90] Han Y, Gao B, Wu G, Huo J, Chen B, Li Y, Guo Y and Liu L 2022 *Opt. Laser Technol.* **148** 107690
[91] Zhang Y, Cui Y, Huang L, Tong L and Liu X 2020 *Opt. Lett.* **45** 6246-6249
[92] Krupa K, Nithyanandan K, Andral U, Tchofo-Dinda P and Grelu P 2017 *Phys. Rev. Lett.* **118** 243901
[93] Zhang Z X, Luo M, Chen J X, Chen L H, Liu M, Luo A P, Xu W C and Luo Z C 2022 *Opt. Lett.* **47** 1750-1753
[94] Tam K K K, Alexander T J, Blanco-Redondo A and Martijn de Sterke C 2019 *Opt. Lett.* **44** 3306-3309
[95] Xu G, Gelash A, Chabchoub A, Zakharov V and Kibler B 2019 *Phys. Rev. Lett*. **122** 084101
[96] Zhang C, Wang J, Gao R, Yang L and Zhang Z 2019 *Optik* **179** 700-707
[97] Zhong X, Chen L, Cheng K, Yao N and Sheng J 2018 *Opt. Express* **26** 15683-15692
[98] Du Y, Xu Z and Shu X 2018 *Opt. Lett.* **43** 3602-3605
[99] Peng J. S., Boscolo S, Zhao Z H and Zeng H P 2019 *Sci. Adv.* **5** 7
[100] Huang Q, Huang Z and Mou C 2021 *Opt. Lett.* **46** 5683-5686
[101] Wei Z W, Liu M, Ming S X, Luo A P, Xu W C and Luo Z C 2018 *Opt. Lett*. **43** 5965-5968
[102] Wang X, Liu Y G, Wang Z, Yue Y, He J, Mao B, He R and Hu J 2019 *Opt. Express* **27** 17729-17742
[103] Huang J, Pang M, Jiang X, He W and Russell P S 2019 *Opt. Express* **27** 26392-26404
[104] Han Y, Gao B, Huo J, Ma C, Wu G, Li Y, Chen B, Guo Y and Liu L 2022 *Chin. Phy. B* **31** 074208.
[105] Deng D, Zhang H, Zu J and Chen J 2021 *Opt. Lett*. **46** 1612-1615
[106] Luo Y, Xiang Y, Shum P P, Liu Y, Xia R, Ni W, Lam H Q, Sun Q and Tang X 2020 *Opt. Express* **28** 4216-4224
[107] Xia R, Luo Y Y, Shum P P, Xiang Y, Ni W J, Liu Y S, Lam H Q, Tang D Y and Tang X H 2020 *IEEE Photon. J.* **12** 1-11
[108] Du W, Li H, Li J, Wang Z, Wang P, Zhang Z and Liu Y presented in part at the Asia Communications and Photonics Conference (ACP) Chengdu Peoples R China 2019
[109] Liu M, Li H, Wei Z W, Li T J, Luo A P, Xu W C and Luo Z C presented in part at the 24th OptoElectronics and Communications Conference (OECC) / International Conference on Photonics in Switching and Computing (PSC) Fukuoka Japan 2019
[110] Du W, Li H, Li J, Wang Z, Zhang Z, Zhang S and Liu Y 2021 *Opt. Express* **29** 14101-14111
[111] Li T J, Liu M, Luo A P, Luo Z C and Xu W C 2020 *Opt. Express* **28** 32010-32018
[112] Du W, Li H, Li J, Wang Z, Zhang Z, Zhang S and Liu Y 2020 *Opt. Lett.* **45** 5024-5027
[113] Cui Y, Zhang Y, Song Y, Huang L, Tong L, Qiu J and Liu X 2021 *Laser Photonics Rev.* **15** 2000216
[114] Du Y, Zeng C, He Z, Gao Q and Mao D 2022 *Chin. Opt. lett.* **20** 011401
[115] Kudelin I, Sugavanam S and Chernysheva M 2020 *Photon. Res*. **8** 776-780
[116] He Z, Zhang C, Wang Z, Chen Y, Liu J and Fan D 2021 *Appl. Phys. Express* **14** 042009

Accepted Manuscript

[117] Wang Z, Wang Z, Liu Y, He R, Zhao J, Wang G and Yang G 2018 *Opt. Lett.* **43** 478-481
[118] Chen H J, Tan Y J, Long J G, Chen W C, Hong W Y, Cui H, Luo A P, Luo Z C and Xu W C 2019 *Opt. Express* **27** 28507-28522
[119] Peng J, Boscolo S, Zhao Z and Zeng H 2019 *Sci. Adv.* **5** eaax1110
[120] Lapre C, Billet C, Meng F, Genty G and Dudley J M 2020 *OSA Continuum* **3** 275-285
[121] Wang X, He J, Mao B, Guo H, Wang Z, Yue Y and Liu Y G 2019 *Opt. Express* **27** 28214-28222
[122] Liu M, Li H, Luo A P, Cui H, Xu W C and Luo Z C 2018 *J. Mod. Optic.* **20** 034010
[123] Wang Z, Wang X, Song Y, Liu J and Zhang H 2020 *Phys. Rev. A* **101** 013825
[124] Peng J, Boscolo S, Tarasov N, Sugavanam S, Churkin D V and Finot C presented in part at the 19th International Conference on Transparent Optical Networks (ICTON) Girona Spain 2017
[125] Liu Y, Luo Y, Xia R, Xiang Y, Ni W, Huang S, Yan Z, Sun Q, Shum P P and Tang X 2021 *Opt. Commun.* **486** 126790
[126] Cao Y, Gao L, Wabnitz S, Ran H, Kong L and Zhu T 2021 *Opt. Laser Technol.* **133** 106512
[127] Wang X, He J, Shi H, Mao B, Feng M, Wang Z, Yue Y and Liu Y G 2020 *Opt. Lett.* **45** 4782-4785
[128] Zhou Y, Ren Y X, Shi J, Mao H and Wong K K Y 2020 *Optica* **7** 965-972
[129] Wu X, Peng J, Boscolo S, Zhang Y, Finot C and Zeng H 2021 *Laser Photonics Rev.* **16** 2100191
[130] Wang P, Xiao X, Grelu P and Yang C 2017 *IEEE Photon. J.* **9** 1-8
[131] Akosman A E and Sander M Y 2018 *Sci. Rep.* **8** 13385
[132] Chen G, Li W, Wang G, Zhang W, Zeng C and Zhao W 2019 *Photon. Res.***7** 187-192
[133] Zheng P Z, Li T J, Xia H D, Feng M J, Liu M, Ye B L, Luo A P, Xu W C and Luo Z C 2021 *Opt. Express* **29** 34684-34694
[134] Peng J, Zhao Z, Boscolo S, Finot C, Sugavanam S, Churkin D V and Zeng H 2021 *Laser Photonics Rev.***15** 2000132
[135] Suzuki M, Boyraz O, Asghari H and Jalali B 2020 *Sci. Rep.***10** 14460
[136] Gurevich S V, Schelte C and Javaloyes J 2019 *Phys. Rev. A* **99** 061803(R)
[137] Albers T, Cisternas J and Radons G 2019 *New J. Phys.* **21** 103034
[138] Descalzi O, Cartes C, Cisternas J and Brand H R 2011 *Phys. Rev. E* **83** 056214
[139] Soto-Crespo J, Akhmediev N and Chiang K 2001 *Phys. Lett. A* **291** 115-123
[140] Akhmediev N and Soto-Crespo J M 2003 *Phys. Lett. A* **317** 287-292
[141] Mou D S, Fang J J and Fan Y 2021 *Optik* **244** 167554
[142] Akhmediev N and Soto-Crespo J M 2004 *Phys. Rev. E* **70** 036613
[143] Descalzi O and Brand H R 2010 *Phys. Rev. E* **82** 026203
[144] Soto-Crespo J M and Akhmediev N 2005 *Math. Comput. Simulat.* **69** 526-536
[145 Cartes C and Descalzi O 2016 *Phys. Rev. A* **93** 031801(R)
[146] Cartes C, Descalzi O and Brand H R 2012 *Phys. Rev. E* **85** 015205
[147] Descalzi O and Cartes C 2017 *Applied Sciences* **7** 887
[148] Cartes C, Descalzi O and Brand H R 2019 *Phys. Rev. E* **100** 012214
[149] Cisternas J and Descalzi O 2013 *Phys. Rev. E* **88** 022903
[150] Latas S C V and Ferreira M F S 2020 *Fiber Integrated Opt.* **39** 273-285
[151] Descalzi O and Brand H R 2018 *Chaos* **28** 075508
[152] Cartes C and Descalzi O 2015 *Fiber Integrated Opt.* **34** 14-22
[153] Latas S C V and Ferreira M F S 2010 *Opt. Lett.* **35** 1771-1773
[154] Latas S C V and Ferreira M F S 2011 *Opt. Lett.* **38** 3085-3087
[155] Hajizadeh Nazari S and Arabanian A S 2018 *J. Opt. Soc. Am. B* **35** 2633-2641
[156] Du W, Li H, Li J, Wang Z and Liu Y presented in part at the 18th International Conference on Optical Communications and Networks (ICOCN) Huangshan Peoples R China 2020
[157] Meng F, Lapre C, Billet C, Genty G and Dudley J M 2020 *Opt. Lett.* **45** 1232-1235
[158] Dutta Gupta B, Das Chowdhury S, Dhirhe D and Pal M 2020 *J. Opt. Soc. Am. B* **37** 2278-2286
[159] Du Y and Shu X 2018 *Opt. Express* **26** 5564-5575
[160] Du Y, Han M and Shu X 2020 *Opt. Lett.* **45** 666-669
[161] Cundiff S T, Soto-Crespo J M and Akhmediev N 2002 *Phys. Rev. Lett.* **88** 073903
[162] Peng J, Boscolo S, Zhao Z and Zeng H presented in part at the 22nd International Conference on Transparent Optical Networks (ICTON) Bari Italy 2020
[163] Wei Z W, Liu M, Ming S X, Cui H, Luo A P, Xu W C and Luo Z C 2020 *Opt. Lett.* **45** 531-534
[164] Han M, Li X, Zhang S, Yan D, Liu J, Han H and Yang Z 2019 *IEEE J. Sel. Topics Quantum Electron.* **25** 1-6
[165] Liu M, Luo A P, Xu W C and Luo Z C presented in part at the Progress in Electromagnetic Research Symposium (PIERS) Shanghai Peoples R China 2016
[166] Peng J, Sorokina M and Zeng H 2021 *J. Lightwave Technol.* **39** 6579-6584
[167] Krupa K, Nithyanandan K and Grelu P 2017 *Optic* **4** 1239-1244
[168] Yu Y, Luo Z C, Kang J and Wong K K Y 2018 *Opt. Lett.* **43** 4132-4135

Accepted Manuscript

[169] Wang P, Xiao X, Zhao H and Yang C 2017 *IEEE Photon. J.* **9** 1507008

[170] Xiao X presented in part at the 16th International Conference on Optical Communications and Networks (ICOCN) Wuzhen Peoples R China 2017

[171] Das Chowdhury S, Dutta Gupta B, Chatterjee S, Sen R and Pal M 2020 *J. Mod. Optic.* **22** 065505

[172] Liu M, Li T J, Luo A P, Xu W C and Luo Z C 2020 *Photon. Res*. **8** 246-251

[173] Peng J and Zeng H 2019 *Commun. Phys-UK* **2** 1-8

[174] Runge A F J, Broderick N G R and Erkintalo M 2016 *J. Opt. Soc. Am.B-Opt. Phy*. **33** 46-53

[175] Peng J and Zeng H 2019 *Phys. Rev. Appl.* **12** 034052

[176] Runge A F J, Broderick N G R and Erkintalo M 2015 *Optica* **2** 36-39

[177] Liu M, Luo A P, Yan Y R, Hu S, Liu Y C, Cui H, Luo Z C and Xu W C 2016 *Opt. Lett.* **41** 1181-1184

[178] Liu M, Luo A P, Xu W C and Luo Z C 2016 *Opt. Lett.* **41** 3912-3915

[179] Zhou Y, Ren Y X, Shi J and Wong K K Y 2020 *Photon. Res.* **8** 1566-1572

[180] Zhou Y, Ren Y X, Shi J and Wong K K Y 2022 *Opt. Lett.* **47** 1968-1971

[181] Ryczkowski P, Närhi M, Billet C, Merolla J M, Genty G and Dudley J M 2018 *Nat. Photonics* **12** 221-227

[182] Zeng J and Sander M Y 2022 *Opt. Express* **30** 7894-7906

[183] Suzuki M, Boyraz O, Asghari H, Trinh P, Kuroda H and Jalali B 2018 *Opt. Lett.* **43** 1862-1865

[184] Igbonacho J, Nithyanandan K, Krupa K, Dinda P T, Grelu P and Moubissi A B 2019 *Phys. Rev. A* **99** 063824

[185] Tchofo Dinda P, Moubissi A B and Nakkeeran K 2001 *Phys. Rev. E* **64** 016608

[186] Kamagate A, Grelu P, Tchofo-Dinda P, Soto-Crespo J M and Akhmediev N 2009 *Phys. Rev. E* **79** 026609

[187] Alsaleh M, Mback C B L, Felenou E T, Dinda P T, Grelu P and Porsezian K 2016 *J. Mod. Optic*. **18** 075501

[188] Pu G, Yi L, Zhang L, Luo C, Li Z and Hu W 2020 *Light-Sci Appl.* **9** 1-8

[189] Kolner B H and Nazarathy M 1989 *Opt. Lett* **14** 630-632

[190] Zhang C, Xu J, Chui P C and Wong K K 2013 *Sci. Rep.* **3** 2064

[191] Zhang Y, Huang L, Cui Y and Liu X 2020 *Opt. Lett.* **45** 4835-4838

[192] Suret P, Koussaifi R E, Tikan A, Evain C, Randoux S, Szwaj C and Bielawski S 2016 *Nature Communications* **7** 13136

[193] Narhi M, Wetzel B, Billet C, Toenger S, Sylvestre T, Merolla J M, Morandotti R, Dias F, Genty G and Dudley J M 2016 Nature Communications **7** 13675

[194] Ma J, Qin Z, Xie G, Qian L and Tang D 2019 *Appl. Phys. Rev.* **6** 021317

Accepted Manuscript